J. Fluid Mech. (2023), *vol*. 977, A42, doi:10.1017/jfm.2023.965

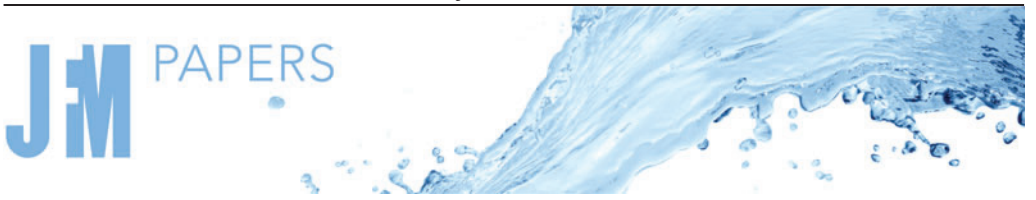

Electromagnetic field effect on a conducting liquid film flowing down an inclined or vertical plane

S. Dholey[1],†, **S. Gorai**[2] **and S. De**[2]

[1]Department of Mathematics, M.U.C. Women's College, Burdwan 713 104, India

[2]Department of Applied Mathematics, University of Calcutta, Kolkata 700009, India

(Received 3 December 2022; revised 14 September 2023; accepted 23 October 2023)

The effect of magnetic as well as electromagnetic fields on the stability of an electrically conducting viscous liquid film flowing down an inclined plane has been investigated for the full range of inclination angles θ ($0 < \theta \leq 90^\circ$) in association with a given value of the Reynolds number Re ($0 < Re \leq 100$), and vice versa. A nonlinear evolution equation is derived by using the momentum-integral method, which is valid for both small and large values of Re. Use of the normal mode approach on the linearized surface evolution equation gives the stability criterion and the critical value of the wavenumber k_c (for which the imaginary part of the complex frequency ω_i^+ is zero) which conceive the electric parameter E, magnetic parameter M, Reynolds number Re, Weber number We and inclination angle θ. The nonlinear stability analysis based on the second Landau constant J_2 helps to demarcate all four possible distinct flow zones (explosive, supercritical, unconditional and subcritical) of this problem. A novel result of this analysis is a simple relationship between the critical values of k_c and k_j (for which J_2 is zero) that basically gives the necessary conditions for the existence of the range of k for an explosive unstable zone, which is either one or two accordingly as $k_j > k_c$ or $k_j < k_c$, and the non-existence of an unconditional stable zone is $k_j \leq k_c$ depending upon the values of M. The analysis confirms the existence of two critical values of M, namely, M_c (for which k_c is zero) and M_j (for which k_j is zero). Here, $M_j > M_c$ except for $\theta = 90^\circ$; and we have found the existence of all four or two (unconditional and subcritical) or one (subcritical) zone(s) of this flow problem accordingly, as $0 \leq M < M_c$ or $M_c \leq M < M_j$ and $M > M_j$ or $M = M_j$.

Key words: thin films, Navier–Stokes equations, nonlinear instability

† Email address for correspondence: sdholey@gmail.com

1. Introduction

The stability problem of a liquid film flowing down an inclined or vertical plane is of increasing importance owing to its widespread applications in various areas of applied science and engineering, such as in heavy casting technology, precision coating, laser cutting processes and the processes of paint finishing, etc. A microscopic instability can cause catastrophic conditions for the film flow problems, therefore it is desirable to investigate this flow problem properly and accurately for making successful designs of fluid devices so that homogeneous fluid flow as per the required conditions can be made. Here, it is important to mention that enormous mathematical calculations, as well as various numerical programs that are required for exploring this type of flow problem theoretically or experimentally, must be correct.

Kapitza & Kapitza (1949) were the first to investigate experimentally the wave motions of a viscous fluid layer flowing down a vertical cylinder, where they recorded the existence of several wavy regimes, including a series of nearly solitary waves. After this pioneering work, several experimental studies on liquid films flowing down an inclined or vertical plane under various conditions have been carried out by many researchers (e.g. Ishihara, Iwagaki & Ishihara 1952; Greenberg 1956; Binnie 1957, 1959; Fulford 1964; Massot, Irani & Lightfoot 1966; Whitaker & Jones 1966; Liu, Paul & Gollub 1993; Liu & Gollub 1994; and the references therein). Benjamin (1957) was the first to investigate theoretically the linear instability of a liquid film flowing down an inclined plane being bounded on the other side by a free surface. Yih (1963) presented Benjamin's theoretical results in more simplified forms by considering separately the limits of small Reynolds and small wavenumber. In these analyses, they derived the stability criterion in terms of Reynolds number Re and angle of inclination θ, which fairly agrees with the experimental results for small values of θ (Alekseenko, Nakoryakov & Pokusaev 1994).

Finite-amplitude wave solutions and nonlinear stability analysis of a viscous liquid film flowing down an inclined plane were initiated by Benney (1966). He derived the free-surface evolution equation in terms of film thickness by employing the long-wave expansion method (small Reynolds number approach). Following Benney's analysis, investigation of the long-wave surface evolution equations for various orders of Re and We can be found in the works of Gjevik (1970), Lin (1974), Chang (1989) and Pumir, Manneville & Pomeau (1983), among others. By contrast, the large Reynolds number approach (momentum-integral method) has been employed by Prokopiou, Cheng & Chang (1991) and Lee & Mei (1996) to examine the instability of a viscous liquid film flowing down an inclined plane. It is noticeable that all the above studies are restricted to a definite value of θ or in a specific range of θ in which θ is small. Recently, using the momentum-integral method, Dholey & Gorai (2021) examined thoroughly the linear and nonlinear stability analysis of a viscous liquid film falling down an inclined plane for the full range of the inclination angle θ ($0 < \theta \leq 90^\circ$).

Flow of an electrically conducting liquid film has several practical applications, such as in nuclear energy equipment, different cooling systems and laser cutting processes (Glukhikh, Tananaev & Kirilov 1987; Blum, Mayorov & Tsebers 1989). The effects of an electric field on the falling film problems have been found in the works of Rohlfs *et al.* (2021), Papageorgiou (2019), Tseluiko & Papageorgiou (2006), Wray, Matar & Papageorgiou (2017), and the references therein. Conroy & Matar (2017) investigated the stability of three-dimensional ferrofluid films in a magnetic field. However, there exist many recently published papers on linear and nonlinear stability analysis of an electrically conducting liquid film falling down an inclined or vertical plane. Here, we mention those

by Gonzalez & Castellanos (1996), Korsunsky (1999), Dandapat & Mukhopadhyay (2003), Mukhopadhyay, Dandapat & Mukhopadhyay (2008) and Dholey (2017). Among these studies, only Mukhopadhyay *et al.* (2008) considered the momentum-integral method for investigating the problem under a fixed value $\theta = 75^\circ$. The nonlinear evolution equation (4.5) of our present study may be the same as the corresponding equation (19) in Mukhopadhyay *et al.* (2008), but the results obtained from figures 3–8 of their analysis are not correct, as the curves k_c and k_s (in those figures) do not follow the known relation $k_c = 2k_s$ (Dholey & Gorai 2021). Dandapat & Mukhopadhyay (2003) have shown the existence of two critical values of M, namely, M_c and $\bar{M}_c$, in figure 3 of their analysis. The value of $\bar{M}_c$ (analogous to M_j) is not correct as the curve $J_2 = 0$ decreases continuously with the increase of M (see figures 17 and 18). For this, the present authors claim that the results of Dandapat & Mukhopadhyay (2003) and Mukhopadhyay *et al.* (2008) are of doubtful validity.

The aim of this study is therefore to extend the work of Dholey & Gorai (2021) by considering the flow of an electrically conducting liquid film down an inclined plane in the presence of an electromagnetic field. The linear stability analysis reveals that the magnetic parameter M has a stabilizing influence up to the value $E \approx 2.45$, independent of θ, and after this value of E, the (slowly) destabilizing influence of M has been found up to the value $M \approx 0.73635$, and then continuously follows the stabilizing influence. Here, our main interest in the nonlinear stability analysis is discussed by showing all four possible distinct flow zones of this problem in Re–k, θ–k, E–k and M–k planes. The value of M_j (analogous to $\bar{M}_c \approx 1.253$ of Dandapat & Mukhopadhyay 2003) is obtained numerically as $M_j \approx 3.99730$, independent of the values of E, Re and θ. The novelty of this analysis is the existence of a new explosive unstable zone that arises only in the presence of a magnetic field depending upon the values of the other parameters. The physical reason for this fact has been confirmed by delineating the curves ω_i^+ and J_2 against k for several values of M, since the demarcations of different flow zones of this problem depend essentially on the values (positive or negative) of ω_i^+ and J_2. Various numerical results in the form of figures, especially the range of k for different flow zones of this problem, are presented in the results and discussion sections of this paper to authenticate the solutions and to manifest the effectiveness of the proposed modelling. The non-availability of the experimental evidences does not allow us to compare our numerical results with the experimental predictions.

2. Mathematical formulation

We consider the two-dimensional gravity-driven flow of an electrically conducting viscous fluid layer of mean thickness h_0 down an inclined plane of inclination θ $(0 < \theta \leq 90^\circ)$ with the horizon, in the presence of an electromagnetic field. We introduce a Cartesian coordinates system such that the x-axis coincides with the plane surface, and the z-axis points vertically upwards from this surface, as shown in figure 1. Here, the constant electric and magnetic fields are acting along the normal to the x–z and x–y planes, respectively.

The basic equations governing this flow problem are the continuity equation and the Navier–Stokes equations with the Lorentz (electromagnetic body) force $\boldsymbol{J} \times \boldsymbol{B}$:

$$\boldsymbol{\nabla} \cdot \boldsymbol{v} = 0, \tag{2.1}$$

$$\rho \{\partial_t \boldsymbol{v} + (\boldsymbol{v} \cdot \boldsymbol{\nabla})\boldsymbol{v}\} = -\boldsymbol{\nabla} p + \mu \nabla^2 \boldsymbol{v} + \rho \boldsymbol{g} + \boldsymbol{J} \times \boldsymbol{B}, \tag{2.2}$$

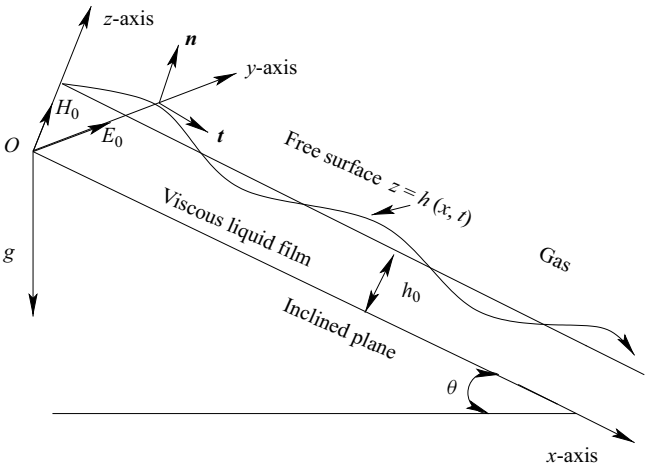

Figure 1. Physical sketch of the problem.

where $\boldsymbol{v} = (u, 0, w)$ and $\boldsymbol{g} = (g\sin\theta, 0, -g\cos\theta)$ are liquid film velocity and gravitational acceleration, respectively, and p, ρ and μ are pressure, density and dynamic viscosity of the fluid, respectively. Here, $\boldsymbol{\nabla} = (\partial_x, 0, \partial_z)$, and ∇^2 is the Laplacian with respect to x and z. The current density $\boldsymbol{J}$ is given by Ohm's law, without the Hall effect as (Shercliff 1965)

$$\boldsymbol{J} = \sigma(\boldsymbol{E} + \boldsymbol{v} \times \boldsymbol{B}), \tag{2.3}$$

where σ is the electrical conductivity of the fluid. The above magnetic and electric fields ($\boldsymbol{B}$ and $\boldsymbol{E}$) are defined by Maxwell's equations as

$$\boldsymbol{\nabla} \cdot \boldsymbol{B} = 0, \quad \boldsymbol{\nabla} \times \boldsymbol{B} = \mu_e \boldsymbol{J} \quad \text{and} \quad \boldsymbol{\nabla} \times \boldsymbol{E} = -\partial_t \boldsymbol{B}, \tag{2.4a–c}$$

where μ_e is the magnetic permeability. We neglect the displacement current in Maxwell's equations since we are not concerned with the consequences that are related in any way to the propagation of electromagnetic waves (Chandrasekhar 1961). As the magnetic Reynolds number is small, one can obtain the electric and magnetic fields as $\boldsymbol{E} = E_0$ and $\boldsymbol{B} = B_0$, respectively (Mukhopadhyay *et al.* 2008; Dholey 2016, 2017; and the references therein).

The boundary conditions related to this flow problem are

$$\boldsymbol{v} = 0 \quad \text{at } z = 0 \quad \text{(no-slip condition)}. \tag{2.5}$$

We define the perturbed interface as $F(x, z, t) = z - h(x, t)$, and then the kinematic condition on the free surface is obtained as (see figure 1)

$$\frac{\mathrm{D}F}{\mathrm{D}t} = \partial_t h + \boldsymbol{v} \cdot \boldsymbol{\nabla}(h - z) = 0 \quad \text{at } z = h(x, t), \tag{2.6}$$

where $\mathrm{D}/\mathrm{D}t$ is the total derivative of the film thickness with respect to time t. Here, the dynamic influence of gas above the liquid film is neglected, and the effect of surface tension is included for which the tangential stress vanishes and the normal stress just

balances with the surface tension:

$$\boldsymbol{\tau}\cdot\boldsymbol{n}\cdot\boldsymbol{t}=0 \quad \text{at } z=h(x,t), \tag{2.7}$$

$$p_0+(\boldsymbol{\tau}\cdot\boldsymbol{n})\cdot\boldsymbol{n}=-\sigma_0\,\boldsymbol{\nabla}\cdot\boldsymbol{n} \quad \text{at } z=h(x,t), \tag{2.8}$$

where $\boldsymbol{n}=(-h_x,1,0)/\sqrt{1+h_x^2}$ and $\boldsymbol{t}=(1,h_x,0)/\sqrt{1+h_x^2}$ are the outward-drawn unit normal and unit tangent vectors to the interface, respectively. Also, $\boldsymbol{\tau}=-pI+2\mu\boldsymbol{e}$ is the stress tensor, where $\boldsymbol{e}=(\boldsymbol{\nabla v}+\boldsymbol{\nabla v}^{\mathrm{T}})/2$ is the rate-of-strain tensor, and $\boldsymbol{I}$ is the identity tensor. Moreover, p_0 is the pressure of the ambient gas and σ_0 is the surface tension coefficient.

To rewrite the basic equations and the boundary conditions in dimensionless form, we introduce the dimensionless variables with a bar sign as

$$x=l_0\bar{x},\quad (h,z)=h_0(\bar{h},\bar{z}),\quad t=(l_0/u_0)\bar{t},\quad u=u_0\bar{u},\quad w=(u_0h_0/l_0)\bar{w},\quad p=(\rho u_0^2)\bar{p}, \tag{2.9a–f}$$

where we consider l_0 as the characteristic longitudinal length scale whose order may be considered the same as the wavelength, h_0 as the length scale in the transverse direction and the Nusselt velocity $u_0=gh_0^2\sin\theta/3\nu$ as the velocity scale along the longitudinal direction.

Using (2.9*a–f*) in (2.1)–(2.8), removing the bar sign over the variables, and retaining the terms up to $O(\epsilon)$, we obtain the reduced governing hydromagnetic equations as

$$u_x+w_z=0, \tag{2.10}$$

$$\epsilon\,Re\,(u_t+uu_x+wu_z)=-\epsilon\,Re\,p_x+u_{zz}+3+M^2(E-u), \tag{2.11}$$

$$0=-Re\,p_z-3\cot\theta+\epsilon w_{zz}. \tag{2.12}$$

The reduced boundary conditions at the plate surface ($z=0$) are

$$u=0 \quad \text{and} \quad w=0, \tag{2.13a,b}$$

and on the free surface ($z=h(x,t)$) are

$$w=h_t+uh_x, \tag{2.14}$$

$$u_z=0 \tag{2.15}$$

and

$$p-p_a+\epsilon^2\,We\,h_{xx}=0. \tag{2.16}$$

The dimensionless parameters associated with this problem are as follows: $\epsilon=h_0/l_0$ is the aspect ratio, which is very small ($\ll 1$) as the fluid film is thin; $Re=u_0h_0/\nu$ is the Reynolds number, which measures the strength of the Nusselt flow; $M=B_0h_0\sqrt{\sigma/\rho\nu}$ is the Hartmann number, which measures the strength of the magnetic field; $E=E_0/(B_0u_0)$ is the electric parameter, which measures the strength of the electric field; $p_a=p_0/(\rho u_0^2)$ is the atmospheric pressure; and $We=\sigma_0/(\rho u_0^2h_0)$ is the Weber number, which measures the surface tension.

Indeed, the strength of the parameters E, M, Re and We can vary widely depending upon numerous factors, including the types of fluids, angle of inclination θ, flow layer thickness h_0, source values of B_0 and E_0, and the specific conditions of the environment. However, to estimate the realistic physical values of the parameters E, M, Re and We for the most

Fluid	u_0 (m s^{-1})	E	M	Re	We
Mercury at 20 °C	0.07250	1.37934	0.77619	37.92423	113.892407
Liquid sodium at 400 °C	0.02928	3.41528	3.04225	6.18596	3656.39321

Table 1. Values of E, M, Re and We for different electrically conducting fluids.

common electrically conducting fluids, such as mercury and liquid sodium, we have taken $g = 9.8$ m s^{-2}, $h_0 = 0.6 \times 10^{-4}$ m, $\theta = 45°$, $E_0 = 0.05$ V m^{-1} and $B_0 = 0.5T$, and then computed the values of E, M, Re and We presented in table 1. It is well known that for mercury at 20 °C, $\rho = 13545$ kg m^{-3}, $\nu = 1.147 \times 10^{-7}$ m^2 s^{-1}, $\sigma = 1.04 \times 10^6$ S m^{-1} and $\sigma_0 = 0.4865$ N m^{-1}; and for liquid sodium at 400 °C, $\rho = 856$ kg m^{-3}, $\nu = 2.840 \times 10^{-7}$ m^2 s^{-1}, $\sigma = 2.50 \times 10^6$ S m^{-1} and $\sigma_0 = 0.1610$ N m^{-1}. Observing the values of E, M, Re and We, we have assumed that $E \approx O(1) \approx M$, $Re \approx O(\epsilon^{-1})$ and $We \approx O(\epsilon^{-2})$.

The nonlinear system of equations (2.10)–(2.16) admits a steady basic solution $(u, w) \equiv (U, 0)$, independent of x and t, which is obtained as follows:

$$u(z) = \frac{1}{\delta_1}\left(\frac{m}{h}\right) U(Z), \tag{2.17}$$

where

$$\left.\begin{aligned} U(Z) = \frac{a_0}{M^2}\left(1 - \frac{\cosh\{M(Z-1)\}}{\cosh(M)}\right), \quad m = \int_0^h u\,\mathrm{d}z = \frac{a_0 h}{M^2}\left(1 - \frac{\tanh(Mh)}{Mh}\right) \\ \text{and} \quad \delta_1 = \int_0^1 U(Z)\,\mathrm{d}Z = \frac{a_0}{M^2}\left(1 - \frac{\tanh M}{M}\right), \quad \text{with } a_0 = 3 + EM^2 \text{ and } Z = \frac{z}{h}. \end{aligned}\right\} \tag{2.18}$$

Equations (2.11) and (2.18) confirm that the magnetic field can be applied without any electric field, but the electric field acts only in the presence of a magnetic field. In fact, the electromagnetic field in a fluid medium is the combination of an electric field with a magnetic field. For $E = 0$ and $M \to 0$, $U(Z) \to (3Z - 1.5Z^2)$ as well as $(m, \delta_1) \to (h^3, 1)$, which are exactly the same as the corresponding results reported by Dholey & Gorai (2021).

3. Momentum-integral equations

Integrating (2.12) and then using (2.16), we obtain the dimensionless pressure $p(x, z, t)$ as

$$p = p_a - \epsilon^2\, We\, h_{xx} + 3\, Re^{-1} \cot\theta\,(h - z). \tag{3.1}$$

Integrating the continuity equation (2.10) and the x-momentum equation (2.11), after using (3.1), with respect to z from 0 to h by the Leibnitz rule, and using the boundary conditions (2.13a,b)–(2.15), we have

$$h_t + m_x = 0, \tag{3.2}$$

$$m_t + \alpha\left(\frac{m^2}{h}\right)_x = \epsilon^2\, We\, hh_{xxx} - \left(\frac{3\cot\theta}{Re}\right) hh_x + \frac{3h}{\epsilon\, Re} - \frac{Am}{\epsilon\, Re\, h^2} - \frac{M^2}{\epsilon\, Re}(Eh - m), \tag{3.3}$$

where the expressions of the shape factors A and α are given by

$$\left.\begin{gathered} A = \left(\frac{\mathrm{d}U}{\mathrm{d}Z}\right)_{Z=0} = M^2\left(\frac{\tanh M}{M-\tanh M}\right) \quad \text{and} \quad \alpha = \frac{\delta_2}{\delta_1^2} = \frac{M}{2}\,\frac{3(M-\tanh M)-M\tanh^2 M}{(M-\tanh M)^2}, \\ \text{with } \delta_2 = \int_0^1 U^2(Z)\,\mathrm{d}Z. \end{gathered}\right\} \tag{3.4}$$

Equation (3.4) confirms that the shape factors A and α depend only on the values of M. For $M \to 0$, $(A, \alpha) \to (3.0, 1.2)$, which are exactly the same as the values obtained by Dholey & Gorai (2021). The full range of α can be obtained as $1 \le \alpha \le 1.2$ since $\alpha \to 1$ as $M \to \infty$.

Equations (3.2) and (3.3) have a known solution

$$m_0 = \delta_1 = \frac{a_0}{M^2}\left(1 - \frac{\tanh M}{M}\right), \quad h = 1, \tag{3.5}$$

which is the Nusselt flat-film solution in the presence of an electromagnetic field, which has the property that as $M \to 0$, $m_0 \to 1$ irrespective of the values of E.

4. Stability analysis

The results of both linear and nonlinear stability analysis will be deduced from the free surface evolution equation. To obtain the nonlinear evolution equation of this problem, we assume

$$h(x,t) = 1 + \eta(x,t) \quad \text{and} \quad m(x,t) = m_0 + \bar{m}(x,t), \tag{4.1a,b}$$

where $\eta \ll 1$ and $\bar{m} \ll 1$ are the dimensionless perturbations of the film thickness and flow rate, respectively. Substituting (4.1*a*,*b*) into (3.2) and (3.3), retaining the terms up to the second-order fluctuations, and then dropping the bar sign, we get

$$\eta_t + m_x = 0, \tag{4.2}$$

$$\begin{aligned} m_t + \alpha\left(2m_0 m_x - m_0^2\eta_x\right) - \epsilon^2\, We\,\eta_{xxx} + \left(\frac{3\cot\theta}{Re}\right)\eta_x - \left\{\frac{9+M^2(3E-2m_0)}{\epsilon\, Re}\right\}\eta \\ + \frac{(A+M^2)m}{\epsilon\, Re} = -2m_t\eta - 2\alpha(mm_x + m_0 m_x\eta - m_0\, m\eta_x) - \left(\frac{9\cot\theta}{Re}\right)\eta\eta_x \\ + \left\{\frac{9+M^2(3E-m_0)}{\epsilon\, Re}\right\}\eta^2 - \left(\frac{2mM^2}{\epsilon\, Re}\right)\eta + 3\epsilon^2\, We\,\eta\eta_{xxx}. \end{aligned} \tag{4.3}$$

Assuming $O(m) = O(\eta) = \epsilon$, we obtain the zeroth-order approximation from (4.3) as

$$m = c\eta \quad \text{with } c = \frac{9+M^2(3E-2m_0)}{A+M^2}, \tag{4.4}$$

which is the linear phase velocity that depends highly on the values of E and M. For $M \to 0$, whatever may be the value of E, (4.4) takes the form $m = 3\eta$, which is exactly the same as reported by Alekseenko *et al.* (1994) and Dholey & Gorai (2021).

Differentiating (4.3) with respect to x, eliminating m for linear terms by using (4.2) and for nonlinear terms by using the relationship $\partial_t = -c\,\partial_x$ obtained from (4.2) and (4.4),

making the transformation $(x, t) = \epsilon(\tilde{x}, \tilde{t})$, and finally dropping the tilde sign, the nonlinear evolution equation in terms of η is obtained as

$$\eta_t + a_1\eta_x + a_2\eta_{tt} + a_3\eta_{xt} + a_4\eta_{xx} + a_5\eta_{xxxx} + a_6\eta\eta_x + a_7\eta\eta_t + a_8(\eta\eta_t)_t + a_9(\eta\eta_x)_x + a_{10}(\eta\eta_{xxx})_x = 0, \tag{4.5}$$

where the expressions of the unknown coefficients a_1–a_{10} are obtained as follows:

$$\left.\begin{gathered} a_1 = \frac{9 + M^2(3E - 2m_0)}{A + M^2} = c, \quad a_2 = \frac{Re}{A + M^2}, \quad a_3 = \frac{2\alpha\, Re\, m_0}{A + M^2}, \\ a_4 = \frac{Re}{A + M^2}(\alpha m_0^2 - 3\, Re^{-1}\cot\theta), \quad a_5 = \frac{Re\, We}{A + M^2}, \quad a_6 = \frac{18 + M^2(6E - 2m_0)}{A + M^2}, \\ a_7 = \frac{4M^2}{A + M^2}, \quad a_8 = \frac{2\, Re\,(1 - \alpha)}{A + M^2}, \quad a_9 = -\frac{9\cot\theta}{A + M^2}, \quad a_{10} = \frac{3\, Re\, We}{A + M^2}. \end{gathered}\right\} \tag{4.6}$$

The nonlinear evolution equation for an incompressible viscous fluid was derived by Dholey & Gorai (2021) (see their equation (29)) where they presented the same equation in the format as (4.5) for the present study. For $M \to 0$, $a_7 \to 0$, (4.5) corroborates (29) of Dholey & Gorai (2021) after reducing one of the subscript values of the coefficients a_8, a_9 and a_{10}. It is noticeable that each and every coefficient of (4.5) conceives the magnetic parameter M, while the electric parameter E has been involved only with the coefficients a_1, a_3, a_4 and a_6. This phenomenon confirms that the magnetic as well as the electromagnetic field has a significant impact on the linear as well as on the nonlinear stability of the thin film flow problems. Therefore, the objective of the present study is to estimate the effects of E and M in association with Re and θ on the linear as well as on the nonlinear stability analysis of an electrically conducting liquid film flowing down an inclined or vertical plane.

4.1. *Results and discussion for linear stability analysis*

In this subsection, we will examine the linear response of the film flow by assuming the sinusoidal perturbation in the form

$$\eta = \Lambda \exp[\mathrm{i}(kx - \omega t)] + \text{c.c.}, \tag{4.7}$$

where Λ is the amplitude of the disturbance, k is the wavenumber, $\omega\ (= \omega_r + \mathrm{i}\omega_i)$ is the complex frequency and c.c. represents the complex conjugate of the term preceding it. Substituting (4.7) into the linearized portion of (4.5), we have

$$D(\omega, k) = -\mathrm{i}\omega + \mathrm{i}a_1 k - a_2\omega^2 + a_3\omega k - a_4 k^2 + a_5 k^4 = 0, \tag{4.8}$$

i.e. the dispersion relation whose solutions are given by

$$\omega^{\pm} = \tfrac{1}{2}\, a_2^{-1}\big[(a_3 k - \mathrm{i}) \pm \sqrt{b + \mathrm{i}d}\big], \tag{4.9}$$

where

$$b = 4a_2(a_5 k^4 - a_4 k^2) + a_3^2 k^2 - 1 \quad \text{and} \quad d = 2(2a_1 a_2 - a_3)k. \tag{4.10a,b}$$

The real and imaginary parts of (4.9) are obtained as

$$\omega_r^{\pm} = \frac{1}{2}a_2^{-1}\left[a_3 k \pm \sqrt{\frac{b+\sqrt{b^2+d^2}}{2}}\right] \quad \text{and} \quad \omega_i^{\pm} = \frac{1}{2}a_2^{-1}\left[-1 \pm \sqrt{\frac{-b+\sqrt{b^2+d^2}}{2}}\right]. \tag{4.11a,b}$$

It is noticeable that ω_i^- is always negative, which gives stability, and ω_i^+ secures stability only when $\omega_i^+ < 0$, which yields the stability criterion

$$Re < 3\cot\theta\left[\left\{\frac{a_0}{M^2}\left(1-\frac{\tanh M}{M}\right)\right\}^2\left\{\left(1+\frac{2\tanh M}{M}\right)^2-\alpha\left(1+\frac{4\tanh M}{M}\right)\right\}-We\,k^2\right]^{-1}. \tag{4.12}$$

The neutral state $\omega_i^+ = 0$ provides the linear phase velocity

$$c_r = \frac{\omega_r}{k} = a_1, \tag{4.13}$$

independent of k, indicating that the wave is non-dispersive, but depends highly on the values of E and M (see (4.6)). When $M = 0$, $c_r = 3$, which coincides with the result reported by Dholey & Gorai (2021). Besides this, the neutral state yields the relations

$$k = 0 \tag{4.14a}$$

and

$$k_c = \sqrt{\frac{\left\{\frac{a_0}{M^2}\left(1-\frac{\tanh M}{M}\right)\right\}^2\left\{\left(1+\frac{2\tanh M}{M}\right)^2-\alpha\left(1+\frac{4\tanh M}{M}\right)\right\}Re-3\cot\theta}{Re\,We}}, \tag{4.14b}$$

which represent the two branches of neutral curves inside which the flow is unstable. The parameters E, Re and θ have a destabilizing influence, while the parameter M has a stabilizing influence on this film flow problem (see figures 4–7). Therefore, the minimum values of E, Re and θ (or M) at which instability (or stability) sets in may be considered as the critical values of the corresponding parameters. For example, the critical value of the Reynolds number Re_c is obtained from (4.14) by putting $k_c = 0$ as

$$Re_c = 3\cot\theta\left[\left\{\frac{a_0}{M^2}\left(1-\frac{\tanh M}{M}\right)\right\}^2\left\{\left(1+\frac{2\tanh M}{M}\right)^2-\alpha\left(1+\frac{4\tanh M}{M}\right)\right\}\right]^{-1}, \tag{4.15}$$

which is highly dependent on the values of θ as well as on the values of E and M. For $M \to 0$ (i.e. in the absence of an electromagnetic field), (4.14) and (4.15) reduce to (38) and (39) of Dholey & Gorai (2021), where they examined the influence of Re and θ on the stability of a viscous liquid film flowing down an inclined or vertical plane. Here, our main objective is to explore how the critical value of any one of the parameters changes with the values of the others, especially for the full range of θ ($0 < \theta \leq 90°$).

Before obtaining the numerical results of this analysis for various values of E, M and θ, we look at the second curly braces term of (4.15), which tends to zero as $M \to 4.62924$, confirming the singularity of Re_c at $M \approx 4.62924$, independent of the values of E and

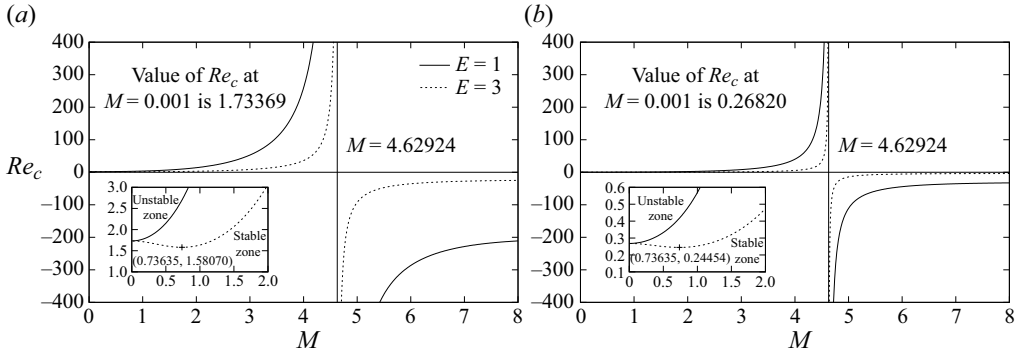

Figure 2. Variation of Re_c with M for some values of E when (*a*) $\theta = 30^\circ$ and (*b*) $\theta = 75^\circ$. For $\theta = 90^\circ$, the value of Re_c is always zero whatever the values of E and M (see (4.15)).

θ ($0 < \theta < 90^\circ$). This result is manifested clearly in figures 2(*a*,*b*), which display the variation of Re_c against M for two distinct values of E (= 1 and 3) when $\theta = 30^\circ$ and 75°, respectively. From these figures, it is easy to say that the realistic (positive) value Re_c will exist up to the value $M \approx 4.62924$. However, this value $M \approx 4.62924$ is practically very large for thin film flow problems since most of the common liquids are poorly conducting. Thus to obtain the numerical results of this problem, we will consider (generally) the value of M, without loss of generality, in the range $0 \leq M \leq 1$ for the ranges $0 \leq E \leq 3$, $0 < Re \leq 100$ and $0 < \theta \leq 90^\circ$. Here, we will consider a fixed value $We = 450$ as it is very large for practical applications.

A noteworthy result that can be found from figures 2(*a*,*b*) is that for a given value of θ ($< 90^\circ$) and up to the value $E \approx 2.45$, the value of Re_c increases continuously with the increase of M, while for a large value of E (above the value $E \approx 2.45$), first the value of Re_c decreases up to a certain minimum (dependent on E and θ) at a certain value of M (e.g. M_m, independent of θ), and then it increases and finally reaches infinity (a very large positive value of Re_c depending upon the values of E and θ) owing to the fulfilment of the singularity condition of Re_c at $M \approx 4.62924$. Hence we can conclude that the magnetic field will show the stabilizing influence on this flow field up to the value $E \approx 2.45$ independent of θ, and after that value it follows (slowly) the destabilizing role but up to the value of M_m, and then continuously follows the stabilizing effect on this flow field. Another remarkable observation that can also be found from these figures is that for a smaller value of E (or θ), the (positive) value of Re_c is always higher than for a larger value of E (or θ), and this result is more pronounced for a higher value of M, confirming the destabilizing influence of E and θ on this flow field. Here, for $E = 3$ and for both values $\theta = 30^\circ$ and 75°, we have found the value $M_m \approx 0.73635$, which will increase for an increasing value of E since it has a destabilizing influence on this flow field.

The magnetic field reduces (depresses) the steady basic flow velocity owing to the formation of the Lorentz resistive force by the interaction of the fluid velocity and the magnetic field inside the flow layer. By contrast, the Lorentz force, which is produced by the electric field (in the presence of a magnetic field), assists the downstream flow, resulting in the enhancement (uplifting) of the basic flow (see (2.11)). Indeed, the depression of the flow velocity causes the increase in the normal pressure on the plate surface, which essentially increases the attachment of the flow to the surface. In the sequel, the frictional force of the adjacent layer to the plate surface increases. Besides this, the

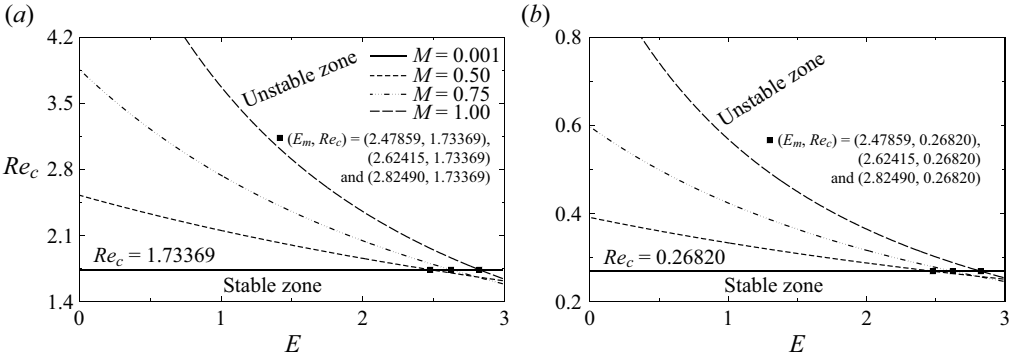

Figure 3. Variation of Re_c with E for several values of M when (*a*) $\theta = 30^\circ$ and (*b*) $\theta = 75^\circ$.

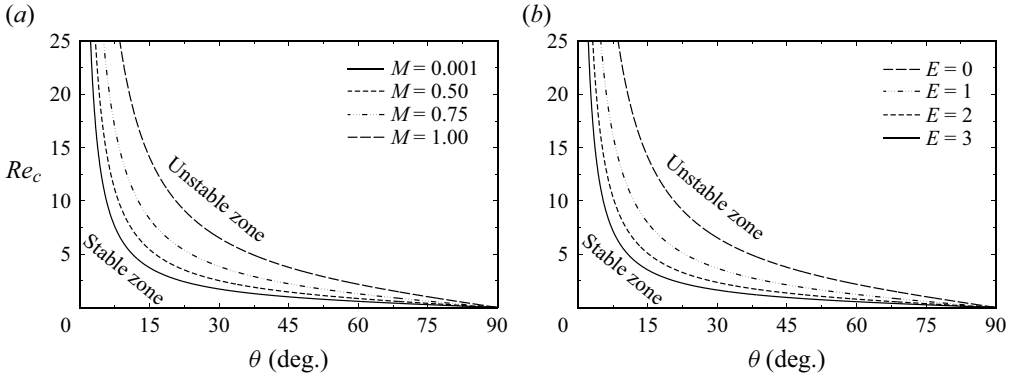

Figure 4. Re_c versus θ for some values of (*a*) M when $E = 0$, and (*b*) E when $M = 1$.

deviation of the mean flow due to the perturbation is suppressed by the magnetic field as the magnetic line of force acts like an elastic string. The combined influence of these two forces stabilizes the liquid film flowing down an inclined plane in the presence of a magnetic field. An opposite explanation holds true for the application of an electric field (in the presence of a magnetic field) in the thin film flow problems. The opposite effects of electric and magnetic field go into competition inside the film flow layers, and ultimately, a mutually stable position originates in between the values of E and M, depending upon the values of θ. In this stable position, the critical value Re_c will be the same for both magnetic and non-magnetic cases. Here, we denote the values of E and M corresponding to the mutually stable position as E_m and M_e. The value of E_m is independent of θ but depends highly on the values of M. Obviously, the value of E_m will be increased with an increasing value of M owing to maintaining this mutually stable position, which one can perceive from figures 3(*a*,*b*). A comparative study of these two figures reveals that the value of Re_c is always lower for a higher value of θ, irrespective of the values of E and M, confirming the destabilizing influence of θ on this flow field.

In order to illuminate the above results more clearly, we depict the variation of Re_c against θ for several values of M and E in figures 4(*a*,*b*), respectively. It is well known that for the non-magnetic case (i.e. for $M = 0$), the value of Re_c decreases continuously with the increase of θ, and ultimately vanishes at $\theta = 90^\circ$ (see figure 3 of Dholey & Gorai 2021). Here, both the parameters E and M follow the above trend but in opposite styles.

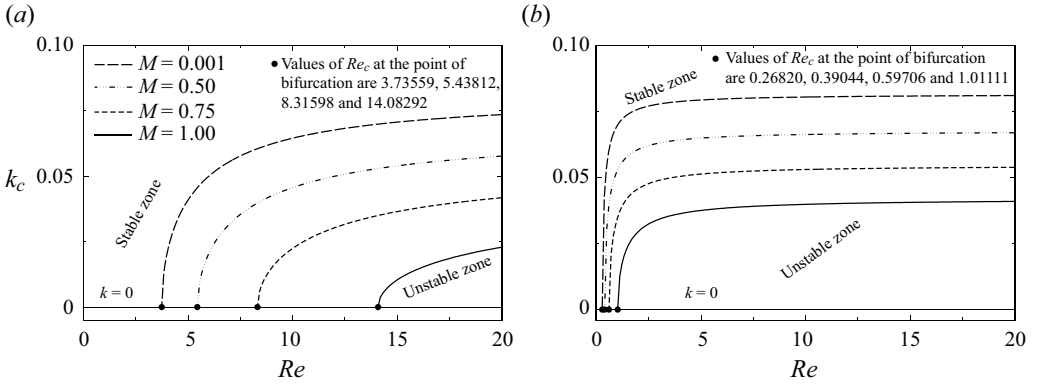

Figure 5. Variation of k_c against Re for four distinct M values at (*a*) $\theta = 15^\circ$ and (*b*) $\theta = 75^\circ$, when $E = 0$. For $\theta = 90^\circ$, the value of k_c is maximum and independent of Re, and we have found $k_c = 0.08161$, 0.06764, 0.05470 and 0.04203 for $M = 0.001$, 0.50, 0.75 and 1.0, respectively.

For any given value of θ $(0 < \theta < 90^\circ)$, the value of Re_c decreases (or increases) continuously with the increase of E (or M), confirming the destabilizing (or stabilizing) influence of E (or M) on this flow field. Besides this, the decreasing (or increasing) rate of Re_c with E (or M) is always higher for a lower value of θ, which confirms the destabilizing effect of θ in the presence of magnetic as well as electromagnetic fields.

The variation of k_c against Re for four distinct values of M (= 0.001, 0.50, 0.75 and 1) is delineated in figures 5(*a*,*b*), corresponding to two fixed values, $\theta = 15^\circ$ and 75°, respectively. Here, we have considered two representative values of θ (= 15° and 75°) from which one can estimate easily the effect of the other values of θ on k_c as well as on Re_c, especially on the stable and unstable zones in the Re–k_c plane, except for $\theta = 90^\circ$, for which $Re_c = 0$ irrespective of the values of E and M, and k_c is independent of Re but depends highly on the values of E and M (see (4.14) and (4.15)). For a given value of θ and for an increasing value of M, the critical value k_c decreases while Re_c increases, resulting in the increase of the linear stable zone, which ensures the stabilizing influence of M on this flow field. The opposite impacts have been found for an increasing value of E, which can be observed readily from figures 6(*a*,*b*). A closer scrutiny at these figures reveals that for given values of E and M, and for an increasing value of θ, the critical value k_c (and hence the linear unstable zone) increases with a concomitant decrease of Re_c. This result ensures that the value of Re_c will be least (zero), and the value of k_c (and hence the linear unstable zone) will be maximum, at $\theta = 90^\circ$, depending upon the values of E and M (see figures 11 and 13). The physical reason behind such behaviour of the flow is the direct involvement of $\cot\theta$ (with a negative sign) in the expression for k_c.

Focusing on the fact that the maximum value of k_c occurs at $\theta = 90^\circ$ independent of Re and dependent on the values of E and M, we plot the variation of k_c against θ for two distinct values of Re (= 1 and 10), and for some values of E and M, in figures 7(*a*) and 7(*b*), respectively. Here, the critical value k_c increases continuously with the increase of θ after reaching the bifurcation point $(\theta_c, 0)$, dependent on the values of E, M and Re, and attains its maximum value at $\theta = 90^\circ$. To maintain the mutually stable position, an increased value of M increases the value of θ_c along with the decrease of k_c resulting in the increase of the linear stable zone. An opposite result has been found for an increasing value of E as well as Re. Finally, we can conclude that the maximum linear unstable zone in

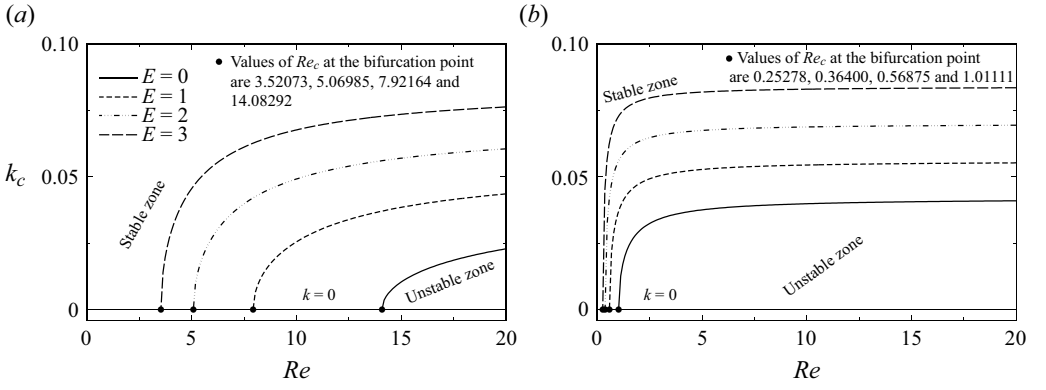

Figure 6. Variation of k_c against Re for four distinct E values at (*a*) $\theta = 15^\circ$ and (*b*) $\theta = 75^\circ$, when $M = 1$. For $\theta = 90^\circ$, the value of k_c is maximum and independent of Re, and we have found $k_c = 0.04203$, 0.05604, 0.07005 and 0.08406 for $E = 0$, 1, 2 and 3, respectively (see (4.14)).

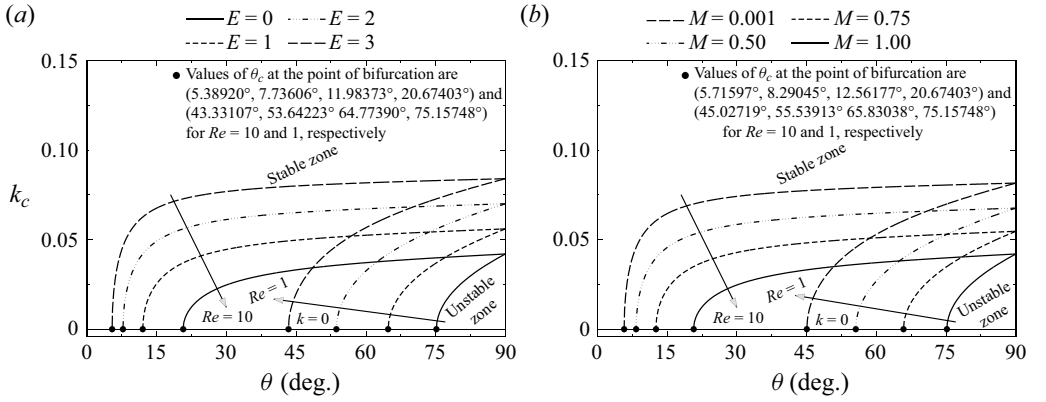

Figure 7. Variation of k_c against θ for two distinct values of Re (= 1 and 10), and for several values of (*a*) E when $M = 1$, and (*b*) M when $E = 0$.

the Re–k plane, as well as the M–k and E–k planes, will be occurring at the value $\theta = 90^\circ$, dependent on the values of E and M, as the cut-off wavenumber k_c is the maximum thereat (see figures 8*a* and 9*a*).

For $M \to 0$ (i.e. for $M = 0.001$), k_c has a fixed value, dependent on Re and θ but independent of E, which decreases continuously with the increase of M, and ultimately vanishes at a definite value of M, for example, M_c depending upon the values of E, Re and θ. Indeed, it is the critical value of M below which the film flow is unstable, and beyond that value the flow will be stable. The above results are manifested clearly in figures 8(*a*,*b*).

Figure 8(*a*) displays the variation of k_c against M for three different values of θ (= 30°, 60° and 90°) corresponding to two fixed values of Re (= 2 and 3) when $E = 0$. For a given value of θ (< 90°) and for an increasing value of Re, the unstable zone increases along with the increase of k_c and M_c owing to its destabilizing impact on this flow field. The unstable zone also increases with the increase of θ, and finally covers the most unstable zone in $\theta = 90^\circ$ independent of the values of Re (see also figure 17*b*). For $\theta = 90^\circ$, k_c is independent of Re but relies on the values of E, M and We (see figures 11 and 13, and (4.14)). Besides this, the term within the second curly braces of (4.14) is zero for $M \approx 4.62924$, independent of the values of E and We (see also figure 2). Hence we see that

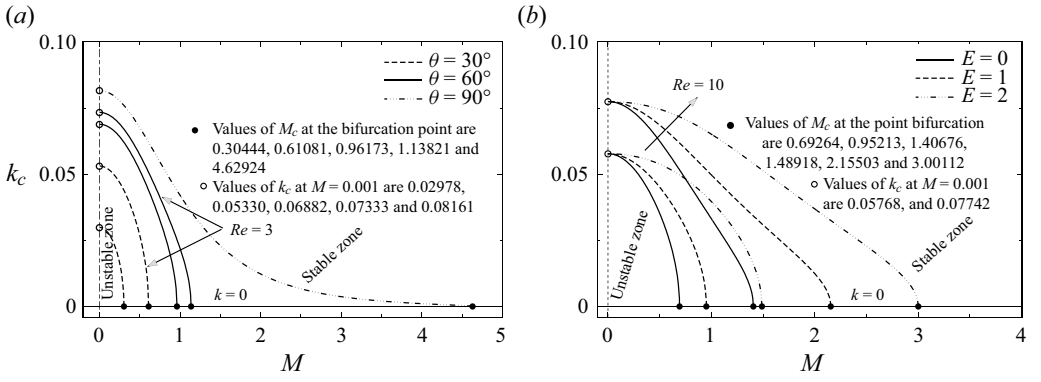

Figure 8. The M–k_c neutral curves for some values of (*a*) Re and θ when $E = 0$, and (*b*) E and Re when $\theta = 45°$. The curve for $\theta = 90°$ is independent of Re. Here, we have considered the values of θ that are greater than $\theta_c \approx 5.71597°$, $18.45127°$ and $26.58679°$ for $Re = 10$, 3 and 2, respectively.

for a vertical plane (i.e. for $\theta = 90°$), the value of k_c will be zero at $M \approx 4.62924$, which is manifested clearly in figure 8(*a*). We have found earlier that the electric field is active only in the presence of a magnetic field. Hence we can conclude that the most unstable zone that occurs in $\theta = 90°$ will be increased (or decreased) with an increasing value of E (or We) without changing the values of k_c (non-magnetic) and M_c, as the parameter E (or We) has a destabilizing (or stabilizing) effect on this flow field.

On the other hand, for given values of Re and θ ($< 90°$), and for an increasing value of E, the unstable zone increases with a concomitant increase of M_c, dependent on Re and θ, but without changing the initial (non-magnetic) values of k_c (which depend on the values of Re and θ), as the electric field effect is zero in the non-magnetic case. These results are manifested clearly in figure 8(*b*). From figures 8(*a*,*b*), it is clear that the value of M_c increases with the increase of E as well as Re and θ owing to their destabilizing influence on this flow field. Here, the stabilizing influence of M balances (neutralizes) the destabilizing influence of the other parameters (E, Re and θ) separately or jointly, and therefore, for an increasing value of any one of the destabilizing parameters, the value of M_c increases. Finally, we conclude that in the presence of an electric field, the magnetic field effect prevails in the competition (means provide only the stable zone) only for a value greater than M_c, while M_c depends on the values of Re and θ.

From the foregoing analysis, it is clear that for the given values of any three of the parameters E, M, Re and θ, the other parameter would have a critical value. Indeed, these are the four mutually critical values in the system for which the total stabilizing and destabilizing influences are balancing each other. To be more precise, a given value of a parameter, whatever may be its effect (stabilizing or destabilizing), and an increasing value of a parameter that has a stabilizing (or destabilizing) influence, essentially increases (or decreases) the parameter, which has a destabilizing influence for adjusting the total stabilizing and destabilizing influences on this flow field. In order to clarify this result, we show the variation of k_c with E for several values of θ and M in figures 9(*a*) and 9(*b*), respectively.

For an increasing value of θ, the critical value E_c decreases continuously, and it becomes zero after a definite value of θ, for example θ_0, that is dependent on M and Re; after this value θ_0, the value of E_c will be negative, which one can guess easily from figure 9(*a*). Here, for $M = 1$ and $Re = 10$, the value of θ_0 is obtained as $\theta_0 \approx 20.6740316°$.

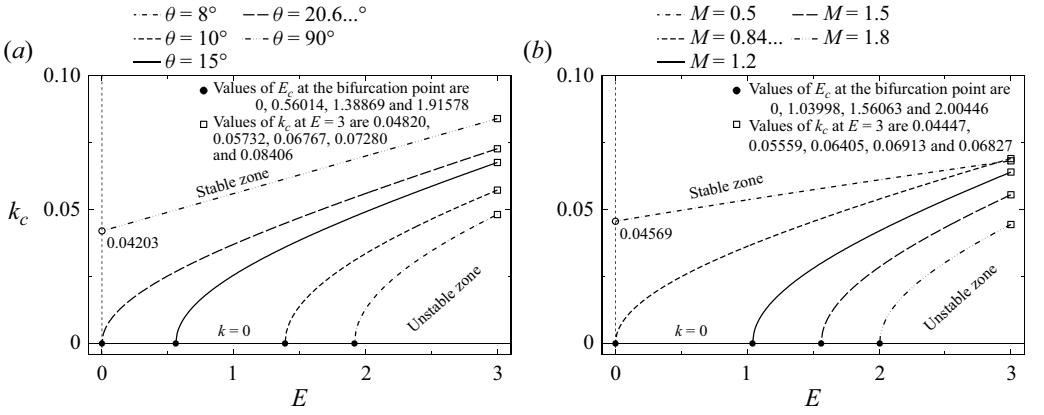

Figure 9. The E–k_c neutral curves for some values of (*a*) θ when $M = 1$, and (*b*) M when $\theta = 15^\circ$, with a fixed value $Re = 10$. Here, we are not presenting the curves k_c for $\theta = 0.2^\circ$, 0.5°, 1°, 2° and 5° for which we have found $E_c = 28.19171$, 16.72716, 10.94868, 6.86170 and 3.23043, respectively.

Besides this, the value of k_c increases with the increase of θ as well as E owing to their destabilizing effect on this flow field. As a result, the unstable zone in the E–k plane increases with the increase of θ, and finally it becomes maximum in $\theta = 90^\circ$. An increased value of θ strengthens the destabilizing influence of the film flow, which essentially decreases the destabilizing influence of E (the value of E_c) for balancing the mutually stable condition owing to the fixed values of other parameters M (= 1) and Re (= 10). Similar results can also be found for an increasing value of Re without changing the values of M and θ since the parameter Re has the same (destabilizing) influence found in the parameter E. And obviously, the opposite phenomenon has been found for an increasing value of M, which is manifested clearly in figure 9(*b*). Here, for $\theta = 15^\circ$ and $Re = 10$, the value of M_0 is obtained as $M_0 \approx 0.84205415$, for which $E_c = 0$. From the above analysis, we come to the conclusion that the linear stable as well as unstable (and hence the range of all four distinct flow) zone(s) of this problem can be controlled easily by adjusting by a suitable amount the parameters E, M, Re and θ.

Dandapat & Mukhopadhyay (2003) examined the stability of a conducting liquid film flowing down an inclined plane in the presence of an electromagnetic field. They have analysed this problem only for the fixed values $Re = 10$ and $\theta = 75^\circ$, and reported that the magnetic field stabilizes the film flow but not for too large values of E. However, the present analysis confirms that the value of E_c is very sensitive (large) especially for the small values of Re and θ in combination with a large value of M, which one can perceive easily from figures 9(*a*,*b*) (see also the figure's caption). Hence their result may be true for some particular values of Re and θ, but not in general, which we have claimed in this paper.

4.2. *Results and discussion for weakly nonlinear stability analysis*

Lin (1974) investigated the finite-amplitude side-band stability of a viscous film flowing steadily down an inclined plane where he stated that in the neighbourhood of the upper branch of the neutral curve $k = k_c$, a thin band of width ς ($\ll 1$) of unstable mode develops over a time $O(\varsigma^{-2})$ and over a distance $O(\varsigma)$ such that $\omega_i^+ \sim O(\varsigma^2)$. This phenomenon ensures that in the marginal state ($\omega_i^+ = 0$), all modes of the perturbation are neither stable

nor unstable, which implies that the linear stability analysis can no longer predict the ultimate behaviour of the flow, therefore the nonlinear stability analysis is necessary for understanding the proper characteristics of the thin film flow down an inclined plane.

Weakly nonlinear stability analysis allows one to examine whether the nonlinear finite-amplitude disturbance in a linear stable zone creates instability (subcritical instability), and the nonlinear evolution of the disturbance decelerates the growth of linear disturbance for which a finite amplitude stable state may arise (supercritical stability), or it accelerates the growth of the linear disturbance, which causes an explosion. Here, we have used the multiple scale method for deriving the complex Ginzburg–Landau type equation (4.5), from which one can characterize easily the proper behaviour of the flow. In order to do this, we consider two sets of mutually independent variables, $(x_1, x_2, \ldots)$ and $(t_1, t_2, \ldots)$, which are

$$x_1 = \varsigma x, x_2 = \varsigma^2 x, \ldots \quad \text{and} \quad t_1 = \varsigma t, t_2 = \varsigma^2 t, \ldots, \tag{4.16a–c}$$

where ς ($\ll 1$) provides the smallness of the corresponding variables. Here, (x, t) are fast scales, while (x_1, t_1), and so on, are slow scales. The temporal and spatial derivatives are obtained as

$$\partial_t \equiv \partial_t + \varsigma\, \partial_{t_1} + \varsigma^2\, \partial_{t_2} + \cdots \quad \text{and} \quad \partial_x \equiv \partial_x + \varsigma\, \partial_{x_1} + \cdots. \tag{4.17a,b}$$

Here, we consider the asymptotic form of the surface elevation $\eta(x, t)$ as

$$\eta(\varsigma, x, x_1, x_2, \ldots, t, t_1, t_2, \ldots) = \varsigma\eta_1 + \varsigma^2\eta_2 + \varsigma^3\eta_3 + \cdots. \tag{4.18}$$

Using (4.16a–c)–(4.18) in (4.5), we get

$$(L_0 + \varsigma L_1 + \varsigma^2 L_2 + \cdots)(\varsigma\eta_1 + \varsigma^2\eta_2 + \varsigma^3\eta_3 + \cdots) = -\varsigma^2 N_2 - \varsigma^3 N_3 - \cdots, \tag{4.19}$$

where $L_0, L_1, L_2, \ldots$ are the operators, and $N_2, N_3, \ldots$ are the nonlinear terms of (4.19), which are given in Appendix A. From (4.19), one can obtain the lowest-order equation of ς as

$$L_0\eta_1 = 0, \tag{4.20}$$

which has a solution of the form

$$\eta_1 = \Lambda(x_1, t_1, t_2)\exp\{\mathrm{i}\Theta\} + \text{c.c.}, \tag{4.21}$$

where $\Theta = kx - \omega_r t$, and c.c. denotes the complex conjugates. The dispersion relation $D(\omega_r, k)$ of (4.21) will be the same as (4.8), except that ω would be ω_r since in the neighbourhood of $k = k_c$, $\omega_i^+ \sim O(\varsigma^2)$, for which $\exp(\omega_i^+ t)$ is slowly varying and may be assimilated in $\Lambda(x_1, t_1, t_2)$.

From (4.19), the second-order equation of ς is obtained as

$$L_0\eta_2 = -L_1\eta_1 - N_2. \tag{4.22}$$

Using (4.21) in (4.22), we get

$$L_0\eta_2 = -\mathrm{i}\left[\frac{\partial D(\omega_r, k)}{\partial \omega_r}\frac{\partial \Lambda}{\partial t_1} - \frac{\partial D(\omega_r, k)}{\partial k}\frac{\partial \Lambda}{\partial x_1}\right]\exp\{\mathrm{i}\Theta\} - Q\Lambda^2\exp\{2\mathrm{i}\Theta\} + \text{c.c.}, \tag{4.23}$$

where $Q = \mathrm{i}(a_6 k - a_7\omega_r) - 2a_8\omega_r^2 - 2a_9 k^2 + 2a_{10}k^4$. From (4.23), the uniform valid solution for η_2 is given by

$$\eta_2 = Q_1\Lambda^2\exp\{2i\Theta\} + \text{c.c.}, \tag{4.24}$$

where $Q_1 = -Q/D(2\omega_r, 2k)$. Introducing the coordinate transformations $\xi = (x_1 - c_g t_1)$ and $\tau = t_2$, where c_g ($= -D_k/D_{\omega_r}$) is the group velocity in the x-direction, and using the

solvability condition in the third-order equation of ς, we have

$$\frac{\partial \Lambda}{\partial \tau} - \frac{\mathrm{i}}{2} c_g'(k) \frac{\partial^2 \Lambda}{\partial \xi^2} - \varsigma^{-2}(F_r + iF_i)\omega_i \Lambda + (J_2 + \mathrm{i}J_4)\,|\Lambda|^2 \Lambda = 0, \tag{4.25}$$

which is the complex Ginzburg–Landau type equation. For $M \to 0$, (4.25) corroborates (49) of Dholey & Gorai (2021) as the values of the coefficients c_g', F_r, F_i, J_2 and J_4 (which are given in Appendix B) reduce to the same as presented in (50) of Dholey & Gorai (2021).

For a filtered wave,

$$\frac{\partial \Lambda}{\partial \tau} - \varsigma^{-2}(F_r + \mathrm{i}F_i)\omega_i \Lambda + (J_2 + \mathrm{i}J_4)\,|\Lambda|^2 \Lambda = 0. \tag{4.26}$$

The solution of (4.26) may be written as

$$\Lambda = a \exp[-\mathrm{i}b(\tau)\,\tau], \tag{4.27}$$

which on substitution in (4.26), and then equating the real and imaginary parts, gives

$$\frac{\partial a}{\partial \tau} = \left(\varsigma^{-2} F_r \omega_i - J_2 a^2\right) a \tag{4.28}$$

and

$$\frac{\partial \{b(\tau)\,\tau\}}{\partial \tau} = \left(J_4 a^2 - \varsigma^{-2} F_i \omega_i\right). \tag{4.29}$$

The sign of J_2 (second Landau constant) that appears in (4.28) due to nonlinearity in the system plays a significant role in determining the varied flow zones of this problem. A positive value of J_2 ensures the saturation of the amplitude of the disturbance, which essentially helps one to delimit the supercritical stability in the linear unstable zone ($\omega_i^+ > 0$) and the unconditional stability in the linear stable zone ($\omega_i^+ < 0$). By contrast, saturation of the amplitude does not occur in a negative value of J_2, which helps one to demarcate the explosive state in the linear unstable zone ($\omega_i^+ > 0$) and the subcritical instability in the linear stable zone ($\omega_i^+ < 0$).

The perturbed wave speed induced by the infinitesimal disturbances appearing in the nonlinear system can be modified by using (4.29). Finally, the threshold amplitude and nonlinear phase velocity are given by

$$\varsigma a = (F_r \omega_i / J_2)^{1/2} \tag{4.30}$$

and

$$Nc_r = c_r + c_i(J_4 F_r / J_2 - F_i), \quad \text{where } c_i = \omega_i / k. \tag{4.31}$$

Mukhopadhyay *et al.* (2008) investigated the influence of an electromagnetic field on the stability of a conducting liquid film flowing down an inclined plane, where they have demarcated four different flow zones of this problem under various values of E and M when $\theta = 75^\circ$ (see figures 3–9 there). However, the demarcations of four different flow zones that are found in their paper are not correct for the following reason. It is noticeable

that the curve J_2 (E, k, M, Re, We, θ), which will be obtained from the relations as given in (B1), has a singular point only when the relationship (singularity condition)

$$\left[\frac{a_0}{M^2}\left(1-\frac{\tanh M}{M}\right)\right]^2\left[\left(1+\frac{2\tanh M}{M}\right)^2-\alpha\left(1+\frac{4\tanh M}{M}\right)\right]Re - 3\cot\theta - 4Re\,We\,k^2 = 0 \tag{4.32}$$

is fulfilled. For given values of any five of the parameters E, k, M, Re, We and θ, (4.32) gives the value of the other at which a singularity of J_2 occurs. For example, if one deals with the values $E = 0$, $M = 0.001$ (i.e. $M \to 0$), $Re = 100$, $We = 450$ and $\theta = 45^\circ$, then one gets $k_s \approx 0.04060$, which completely agrees with the result represented in figure 19(b). From this figure it is clear that below the value of k_s, the curve J_2 is always negative. Besides this, a close relationship between k_s and k_c is obtained from (4.32) and (4.14) as

$$k_s = \frac{1}{2}\sqrt{\frac{\left\{\frac{a_0}{M^2}\left(1-\frac{\tanh M}{M}\right)\right\}^2\left\{\left(1+\frac{2\tanh M}{M}\right)^2-\alpha\left(1+\frac{4\tanh M}{M}\right)\right\}Re - 3\cot\theta}{Re\,We}} = \frac{k_c}{2}, \tag{4.33}$$

which one can check easily from figure 19(a,b). Equation (4.33) ensures that the curve k_s separates the existing linear unstable zone ($\omega_i^+ > 0$) into two equal parts without changing the critical values of Re_c or θ_c or M_c or E_c. Hence the lower region of the curve k_s is entirely an explosive zone as there J_2 is negative, while the upper region may be either wholly a supercritical zone or partly supercritical and partly an explosive zone. This depends on whether the curve $J_2 = 0$ would not cross the curve k_c or cross it (see figures 10–18). From the above analysis, it is confirmed that the graphical representation, especially the demarcations of four different flow zones of this problem presented by Mukhopadhyay *et al.* (2008), are not correct, therefore the results based on these figures have doubtful validity, as claimed earlier.

Considering the relationship (4.33) as well as the signs of ω_i^+ and J_2, we have demarcated all the (correct) four distinct flow zones of this problem in figures 10–18 for the prescribed ranges of E, M and θ. Here, we have included the curves (figures) for $M = 0.001$ (i.e. for $M \to 0$) only to validate the present (non-magnetic) results with the corresponding results reported by Dholey & Gorai (2021) (see figures 6, 10c and 13d there). In comparison, a negligible discrepancy is found owing to consideration of the value $M = 0.001$ instead of $M = 0$.

For the non-magnetic case (i.e. for $M = 0.001$) and for the given values $E = 0$ and $\theta = 45^\circ$, all four distinct zones in the Re–k plane exist only after the critical value Re_c,and all the zones remain practically constant after a certain value of Re as the curves $\omega_i^+ = 0$ and $J_2 = 0$ get their corresponding asymptotic nature after that value of Re (see figure 10a). By contrast, for a given value of M (not too small), the curve $J_2 = 0$ does not follow the asymptotic behaviour with Re, and while following the same asymptotic behaviour, the curve $\omega_i^+ = 0$ depresses gradually towards the Re-axis with a concomitant increase of Re_c for which the unconditional stable zone increases (but up to the value Re_c) along with the decrease of the supercritical stable as well as the explosive unstable zone, which confirms the stabilizing effect of M on this flow field. For a given value of Re, the curve $J_2 = 0$ decreases continuously with the increase of M, resulting in the increase of the subcritical

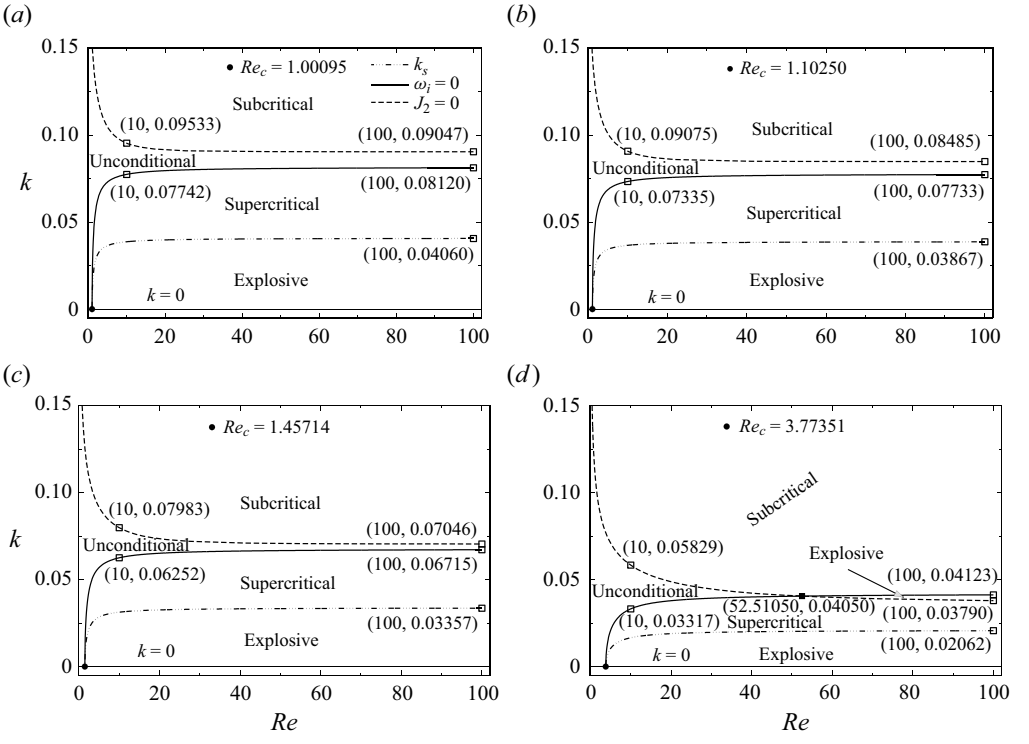

Figure 10. Neutral stability curves in the Re–k plane showing four different flow zones at four different values (*a*) $M = 0.001$, (*b*) $M = 0.25$, (*c*) $M = 0.50$ and (*d*) $M = 1.0$, when $E = 0$, $We = 450$ and $\theta = 45^\circ$. The four different zones found in (*a*) agree well with the corresponding zones reported by Dholey & Gorai (2021) in figure 6 of their analysis. A small discrepancy is found in the values of k and Re_c owing to the consideration of $M = 0.001$ instead of $M = 0$.

unstable zone. The above results are observed directly from figures 10(*b–d*). Here, in the presence of a magnetic field, the curve $J_2 = 0$ decreases continuously with the increase of Re, and finally it crosses the curve $\omega_i^+ = 0$ after a certain value Re_0 of Re, dependent on M, at which the stabilizing influence of M dies out because of the destabilizing influence of Re (see figure 10*d*). Hence we see that the unconditional stable zone of this flow problem will exist only up to the value Re_0, and beyond that value, a new explosive unstable zone will arise that increases with the increase of Re owing to the destabilizing influence of Re on this flow field. Finally, we come to the conclusion that in the presence of a magnetic field, all four distinct flow zones of this problem will exist in a definite range (Re_c, Re_0) of Re, and the unconditional stable zone will vanish after the value Re_0 depending upon the values of E, M and θ.

The corresponding variations of the curves $\omega_i^+ = 0$ and $J_2 = 0$ for a vertical plane (i.e. for $\theta = 90^\circ$) are delineated in figures 11(*a–d*) with the same values of E, M and We as considered in figures 10(*a–d*). In this case, the curve $\omega_i^+ = 0$ is free from Re, and the value of Re_c is zero irrespective of the values of E and M (see (4.14) and (4.15)). By contrast, the curve $J_2 = 0$ depends highly on the values of Re. Here, the parameters M and Re, especially for the curve $J_2 = 0$, follow the same behaviour as we have found in figures 10(*a–d*). A comparative study (of the corresponding parts) of figures 10 and 11 reveals that for an increasing value of θ, the unconditional stable zone decreases along

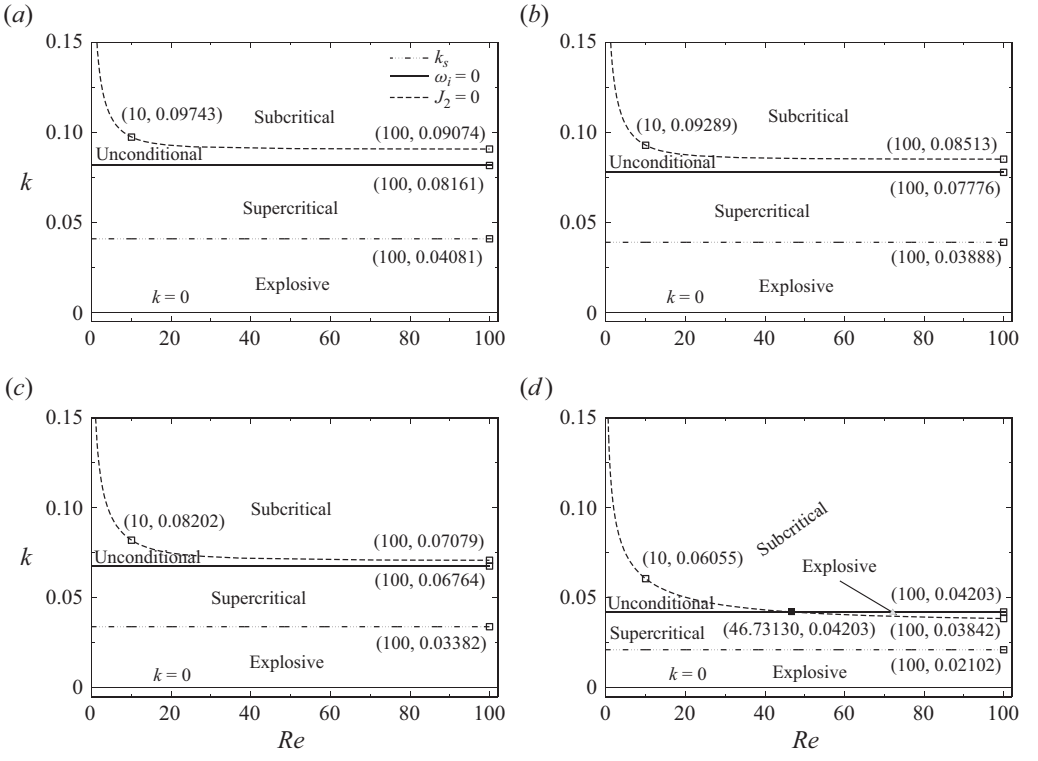

Figure 11. Neutral stability curves in the Re–k plane showing four different flow zones at four different values (*a*) $M = 0.001$, (*b*) $M = 0.25$, (*c*) $M = 0.50$ and (*d*) $M = 1.0$, when $E = 0$, $We = 450$ and $\theta = 90°$. The four different zones found in (*a*) agree well with the corresponding zones reported by Dholey & Gorai (2021) in figure 13(*d*) of their analysis.

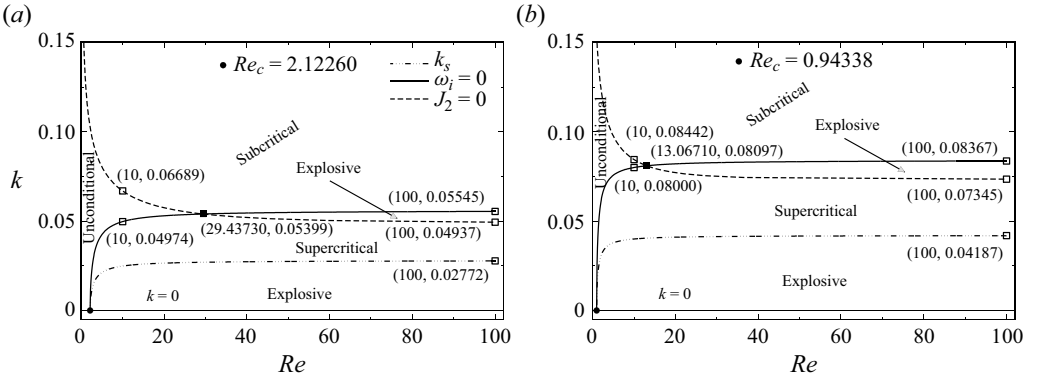

Figure 12. Neutral stability curves in the Re–k plane showing four different flow zones at two different values (*a*) $E = 1$ and (*b*) $E = 3$. The other parameters are chosen as $M = 1$, $We = 450$ and $\theta = 45°$. For $E = 0$, the variation of the same flow zones can be found from figure 10(*d*).

with the increase of the explosive unstable zone. An increased value of θ increases the destabilizing influence in the film flow dynamics, which essentially reduces the existing destabilizing influence of Re for neutralizing the stabilizing influence of M (which is now

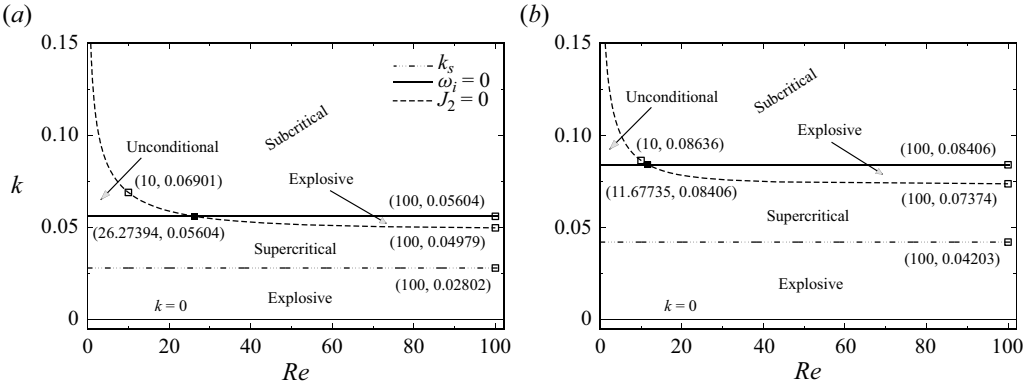

Figure 13. Neutral stability curves in the Re–k plane showing four different flow zones at two different values (*a*) $E = 1$ and (*b*) $E = 3$. The other parameters are chosen as $M = 1$, $We = 450$ and $\theta = 90^\circ$. For $E = 0$, the variation of the same flow zones can be found from figure 11(*d*).

fixed at a given value), resulting in the decrease of the value of Re_0, the upper limit of Re for the existence of four distinct flow zones of this problem.

Next, let us look at figures 12(*a*,*b*), which are depicted for the same values of M, We and θ as considered in figure 10(*d*), and convey the information about the range (Re_c, Re_0) of Re for four distinct flow zones of this problem for various values of E. An increased value of E decreases the values of Re_c and Re_0, indicated on the figures, along with the increase of the values of k_c and k_j. Actually, an inclusion of E enhances the destabilizing influence in the flow system, which is the essential cause of the decrease of Re_c and Re_0 as well as the increase of k_c and k_j. As a result, the unconditional stable zone decreases along with the increase of the explosive unstable zone. Besides this, the new explosive unstable zone arises after the value of Re_0 increases with the increase of E owing to its destabilizing influence on this flow dynamics. Quite notably, if one increases the value of θ without changing the values of other parameters, then one gets more effective results than we have found from figures 12(*a*,*b*) (see figures 13*a*,*b*). When E is added with θ (or θ is increased with a given value of E), they are united and act jointly on the flow system, and the resulting destabilizing influence makes the flow more unstable, which decreases the range (Re_c, Re_0) of Re for four distinct flow zones of this problem.

However, the new information that comes from figures 10–13 is that for an increasing value of M, the unconditional stable zone increases up to the value Re_c, and then decreases and finally vanishes at the value Re_0, depending upon the values of E and θ. Hence, for the given values of E, M and θ, we can divide the whole Re range into the following subintervals, from which one can easily recognize the number of different flow zones of this problem.

(i) For $0 < Re \leq Re_c$, two zones exist, namely subcritical unstable and unconditional stable. This result is true for all values of θ except $\theta = 90^\circ$, for which $Re_c = 0$.
(ii) For $Re_c < Re < Re_0$, all four distinct zones of this flow problem are found for any given value of θ in $0 < \theta \leq 90^\circ$.
(iii) For $Re = Re_0$, all four zones, except the unconditional stable zone, of this flow problem exist for the full range of θ $(0 < \theta \leq 90^\circ)$.
(iv) For $Re_0 < Re \leq 100$, the unconditional stable zone does not exist, while the existence of the other three zones is found for all values of θ considered in the

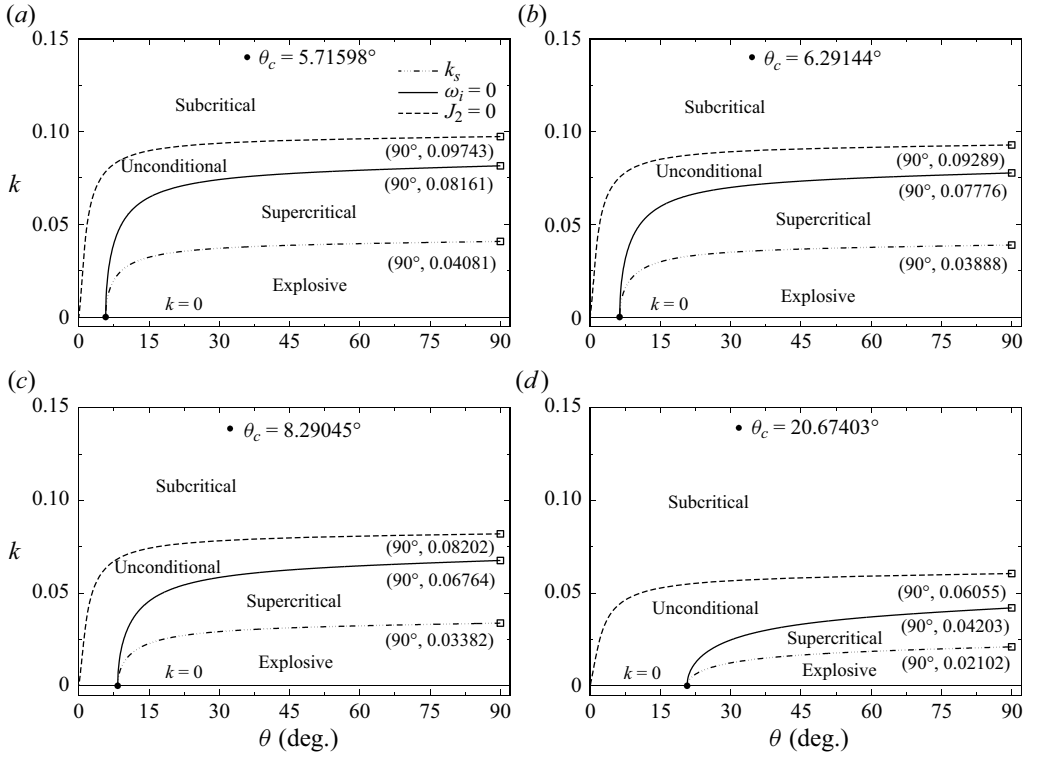

Figure 14. Neutral stability curves in the θ–k plane showing four different flow zones at four different values (*a*) $M = 0.001$, (*b*) $M = 0.25$, (*c*) $M = 0.50$ and (*d*) $M = 1.0$, when $E = 0$, $Re = 10$ and $We = 450$. The four different zones that are found in (*a*) agree well with the corresponding zones reported by Dholey & Gorai (2021) in figure 10(*c*) of their analysis.

present study. Here, a new explosive unstable zone (instead of an unconditional stable zone) originates after the value Re_0, which increases with the increase of E as well as Re and θ.

We conclude our discussion by making some comments on the existence of four distinct flow zones of this problem under various values of the parameters E, M, Re and θ. The relation $k_c = 0$ yields not only the critical value Re_c but also the critical value E_c, as well as M_c and θ_c. The critical value of any one of the parameters E, M, Re and θ can be obtained by imposing the values of the other three parameters into the relation $k_c = 0$, and these are the four mutually critical values of the system. Hence, for a given value of Re in (Re_c, Re_0), there is a critical value θ_c, dependent on the values of E and M, after which the linear instability arises in the flow system and one finds the existence of all four distinct flow zones of this problem (see condition (ii)). Similar results can also be found after the value E_c since both the parameters E and θ have the same (destabilizing) characteristic features on this flow dynamics. By contrast, all four distinct zones of this problem will be found up to the value M_c since the magnetic field has a stabilizing influence on this flow field.

In order to clarify the above results, we have plotted the curves $\omega_i^+ = 0$ and $J_2 = 0$ in the θ–k, E–k and M–k planes for a fixed value $Re = 10$, which obviously belongs to the range $Re_c < Re < Re_0$ for the ranges $0 \leq E \leq 3$, $0 \leq M \leq 1$ and $0 < \theta \leq 90°$ (see

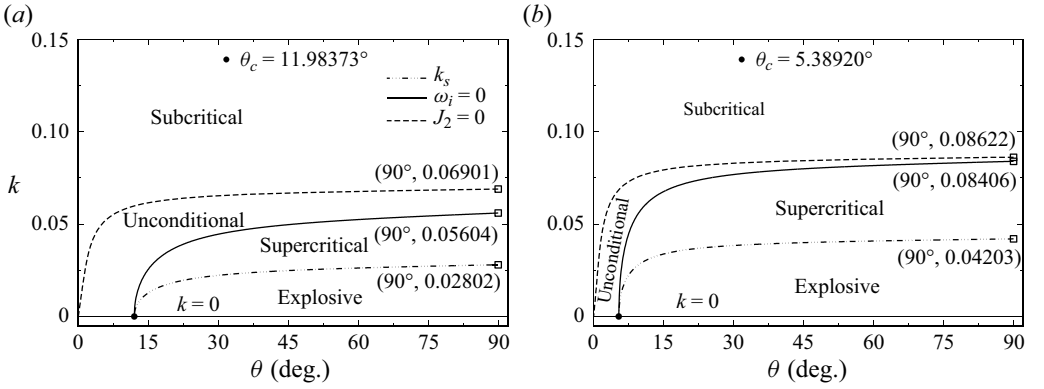

Figure 15. Neutral stability curves in the θ–k plane showing four different flow zones at two different values (*a*) $E = 1$ and (*b*) $E = 3$. The other parameters are chosen as $Re = 10$, $M = 1$ and $We = 450$. For $E = 0$, the variation of the same flow zones can be found from figure 14(*d*).

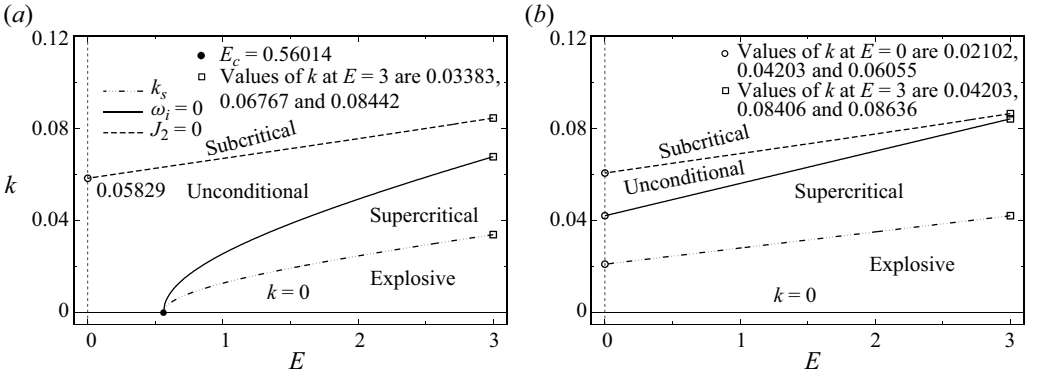

Figure 16. Neutral stability curves in the E–k plane showing four different flow zones at two distinct values (*a*) $\theta = 15°$ and (*b*) $\theta = 90°$, when $M = 1$, $Re = 10$ and $We = 450$.

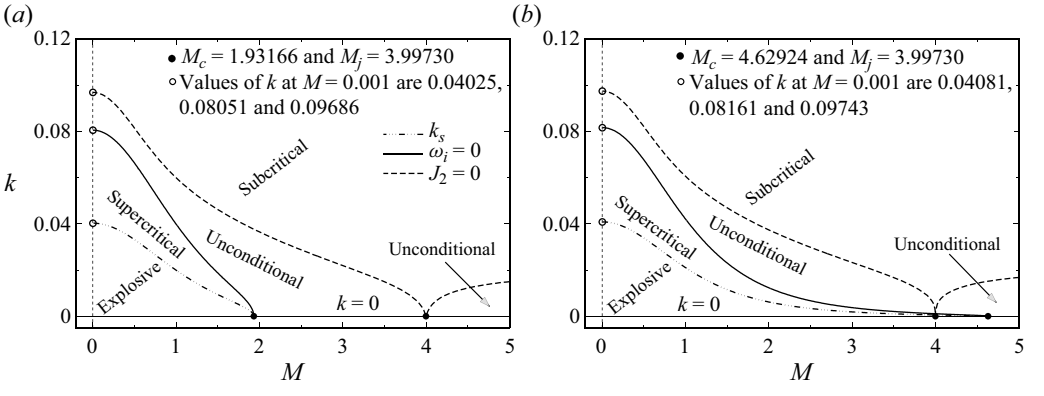

Figure 17. Neutral stability curves in the M–k plane showing four different flow zones at two different values (*a*) $\theta = 75°$ and (*b*) $\theta = 90°$, when $E = 0$, $Re = 10$ and $We = 450$. We have found $M_c \approx 0.84205$ and 1.40676 for $\theta = 15°$ and 45°, respectively.

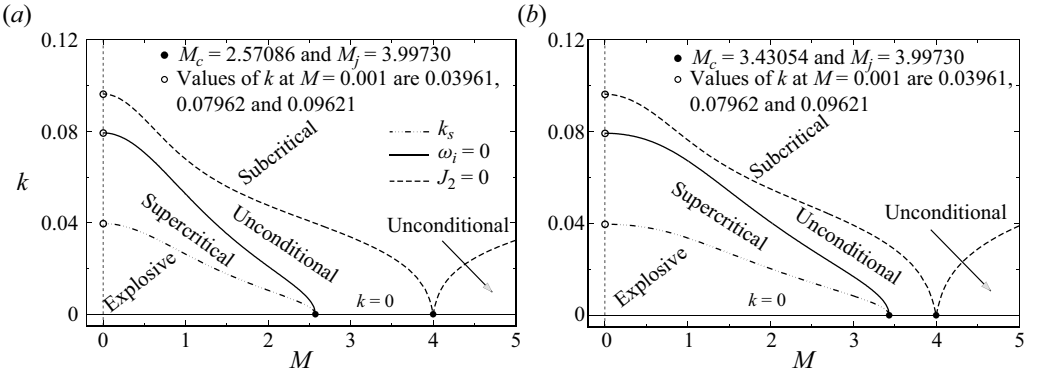

Figure 18. Neutral stability curves in the M–k plane showing four different flow zones at two different values (*a*) $E = 1$ and (*b*) $E = 2$, when $Re = 10$, $We = 450$ and $\theta = 60°$. We have found $M_c = 1.62591$ and 3.90578 for $E = 0$ and 3, respectively.

figures 10–13), in figures 14–18. Figures 14(*a–d*), which are delineated for $E = 0$, show that for a given value of M and for an increasing value of θ, the explosive unstable zone increases after reaching the critical value θ_c, and simultaneously the unconditional stable zone decreases (slowly), confirming the destabilizing impact of θ on this flow dynamics. For an increasing value of M, the curves $\omega_i^+ = 0$ and $J_2 = 0$ depress towards the θ-axis with a concomitant increase of θ_c, resulting in the increase of the unconditional stable zone along with the decrease of the explosive unstable zone, which again confirms the stabilizing influence of the magnetic field on this flow problem. The opposite phenomena have been found for an increasing value of E, which one can perceive easily from figures 14(*d*) and 15(*a*,*b*). This is compatible with the fact that for an increasing value of E as well as θ, the destabilizing influence of the film flow is intensified, and simultaneously the stabilizing influence of M (which is now fixed at a given value) becomes more and more feeble in comparison with the growing destabilizing influence of E and θ.

We have already shown in figure 9(*a*) that for $M = 1$ and $Re = 10$, and for an increasing value of θ, the value of E_c decreases continuously and ultimately vanishes at the value $\theta_0 \approx 20.6740316°$. This phenomenon ensures that for the same values of M and Re, all four distinct zones of this flow problem will exist in the range $E_c < E \leq 3$ or $0 \leq E \leq 3$ of E, accordingly as $\theta < \theta_0$ or $\theta > \theta_0$, as manifested clearly in figures 16(*a*) and 16(*b*), respectively. Here, for a given value of θ, the increasing rate of the critical value k_c (related to the curve $\omega_i^+ = 0$) with E is always higher than that of k_j (related to the curve $J_2 = 0$), resulting in the decrease of the unconditional stable and subcritical unstable zones, with a concomitant increase of the other two zones of this flow problem. This result is more pronounced for a higher value of θ, which confirms our earlier results presented in figures 12, 13 and 15.

Each of figures 10, 11 and 14 ensures that for any given values of E, Re and θ within their prescribed ranges, the curves $\omega_i^+ = 0$ and $J_2 = 0$ decrease continuously with an increasing value of M. This fact confirms that the critical values of k_c (related to the curve $\omega_i^+ = 0$) and k_j (related to the curve $J_2 = 0$) will be zero separately after a definite (generally different) value of M, depending upon the values of E, Re and θ. For this reason, one finds the existence of two distinct critical values of M: one for $k_c = 0$ denoted M_c, and the other

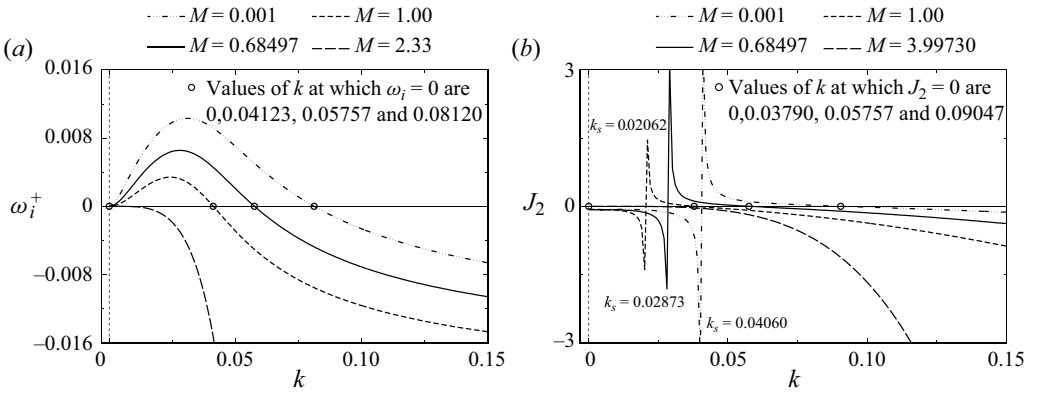

Figure 19. Variation of (*a*) ω_i^+ and (*b*) J_2 with k for some values of M when $E = 0$, $Re = 100$, $We = 450$ and $\theta = 45^\circ$. We have $k_j > k_c$, $k_j = k_c$ or $k_j < k_c$ accordingly as $M < 0.68497$, $M = 0.68497$ or $M > 0.68497$.

for $k_j = 0$ denoted M_j. Focusing on this fact, we plot the curves $\omega_i^+ = 0$ and $J_2 = 0$ in the M–k plane for two fixed values $\theta = 75^\circ$ and 90° when $E = 0$ in figures 17(*a*,*b*), and for two fixed values $E = 1$ and 2 when $\theta = 60^\circ$ in figures 18(*a*,*b*), respectively. A review of these figures discloses that the wavenumber k_j is zero at $M_j \approx 3.99730$ irrespective of the values of E, Re and θ, confirming that the value of M_j is constant for this problem. By contrast, the value of M_c increases continuously with the increase of any one of the parameters E, Re and θ, owing to their destabilizing influence on this flow field. An increased value of θ (or E or Re) increases the value of k_c, which in turn leads to an increase in the value of M_c for vanishing this increased value of k_c (see figures 10, 12 and 14–16). For $\theta = 90^\circ$, the value of $\cot\theta$ is zero, and for $M \approx 4.62924$, the second curly braces term in the expression for k_c is zero (see (4.14)). Hence for the values $\theta = 90^\circ$ and $M \approx 4.62924$, the value of k_c will be zero irrespective of the values of E and Re, which is manifested clearly in figure 17(*b*), confirming our earlier result presented in figure 2.

Now we will explain graphically the reason for the existence of two distinct critical values of M in this problem. For this purpose, we depict the curves ω_i^+ and J_2 against k for some values of M (= 0.001, 0.68497 and 1.0) in figures 19(*a*) and 19(*b*), respectively. For an increasing value of M, the values of k_c and k_j decrease along with the increase of the negative portions of the curves ω_i^+ and J_2. More precisely, we can say that the values of k_c and k_j come close to zero, and the curves ω_i^+ and J_2 depress towards their negative axes. This phenomenon suggests that the values of k_c and k_j will separately be zero (generally) for two distinct (but definite) values of M, ensuring the existence of two critical values of M in this flow problem.

(i) One value of M, for which $k_c = 0$, is denoted by M_c, which depends highly on the values of E, Re and θ. Here, for the given values $E = 0$, $Re = 100$ and $\theta = 45^\circ$, we have obtained $M_c \approx 2.33$, which one can easily and directly appreciate from figure 19(*a*). Interestingly enough, the curve ω_i^+ will be wholly negative after the value of M_c, therefore there is no way for the occurrence of explosive unstable and supercritical stable zones of this flow problem (see figures 17 and 18).

(ii) The other value of M, for which $k_j = 0$, is denoted by M_j, which is obtained as $M_j \approx 3.99730$, independent of the values of E, Re and θ (see figure 19*b*). At the

value M_j, the unconditional stable zone vanishes, and one finds only the existence of a subcritical unstable zone. After the value M_j, a new unconditional stable zone originates in the system that increases (slowly) with the increase of M (see figures 17 and 18).

Dandapat & Mukhopadhyay (2003) examined the stability of a conducting liquid film flowing down an inclined plane in the presence of an electromagnetic field using the long-wave approximation method. They have shown the existence of two distinct critical values of M, namely, M_c and $\bar{M}_c$ in their figure 3, which is same as figure 17(a) of the present study. A comparative study between these two figures reveals that the characteristic features of the curve $\omega_i^+ = 0$ with respect to M are the same; nevertheless, a small discrepancy has been found in the values of M_c due to the employment of different numerical methods. On the contrary, the features of the curve $J_2 = 0$ that are found from figure 17(a) are completely different from those in figure 3 of Dandapat & Mukhopadhyay (2003). From their figure 3, it seems that they have considered the value $\bar{M}_c \approx 1.253$ for which the curve $J_2 = 0$ has a point of discontinuity, which is doubtful. For clarity, we have checked many times the mathematical calculations and the numerical program for the expression of the curve $J_2 = 0$, and finally obtained (tested) the results (numerically) for all values of M ($0 \leq M \leq 5$) in combination with the values of E, Re and θ considered for this study. It is found that the curve $J_2 = 0$ decreases continuously with the increase of M, and finally vanishes at $M_j \approx 3.99730$, independent of the values of E, Re and θ, which is shown in figures 17 and 18. Hence the curve $J_2 = 0$ that was plotted by Dandapat & Mukhopadhyay (2003) in their figure 3 is not correct as claimed.

Finally, we conclude our discussion by stating the reason for the existence of the second range of k for an explosive unstable zone that occurs after the value of Re_0, depending upon the values of E, M, We and θ. Quite notably, this occurs only in the presence of a magnetic field. For $M = 1$, two ranges of k for the explosive unstable zone are found in figures 10–13. The first occurs only when the singularity condition (4.32) of J_2 is fulfilled. Equation (4.33) confirms the existence of a singularity of J_2 at the value $k = k_s$ ($= k_c/2$), below which J_2 is negative and ω_i^+ is positive always, therefore $0 < k < k_s$ is the range of k for an explosive unstable zone generally found in the papers published by the authors concerned (see figures 5 and 12 of Dholey & Gorai 2021).

An increased value of M decreases the values of k_j and k_c in which the decreasing rate of k_j is higher than that of k_c (see figures 19a,b). As a result, the value of k_j crosses the value of k_c after a certain value of M, dependent on E, Re and θ, which obviously follows the relationship

$$k_j \leq k_c. \tag{4.34}$$

(i) When $k_j = k_c$, we denote the parameters related to this case as the same parameters with a zero subscript. For example, if one considers figures 19(a,b), then one gets $k_j = k_c = 0.05757$ for $E_0 = 0$, $M_0 = 0.68497$, $Re_0 = 100$, $We_0 = 450$ and $\theta_0 = 45^\circ$. In this case, the unconditional stable zone vanishes, and one finds the existence of the other three zones of this problem.

(ii) When $k_j < k_c$, a new range $k_j < k < k_c$ of k is found in which J_2 is negative and ω_i^+ is positive always (see figures 19a,b). Indeed, it is the range of k for an explosive unstable zone that newly arises (in place of unconditional stable

zone) under a suitable value of M depending upon the values of the other parameters.

Hence we can conclude that the condition for the existence of the number of the range of k for an explosive unstable zone is one or two accordingly as $k_j > k_c$ or $k_j < k_c$, and for the non-existence of an unconditional stable zone, the condition is $k_j \leq k_c$. Most importantly, the first condition ($k_j > k_c$) occurs in both magnetic and non-magnetic cases, while the other two conditions ($k_j \leq k_c$) occur only in the presence of a magnetic field.

5. Conclusion

We have examined in detail the effect of a magnetic as well as an electromagnetic field on the linear and weakly nonlinear stability of an electrically conducting viscous fluid film flowing down an inclined plane by assuming the magnetic Reynolds number to be small. A normal mode technique and multiple-scale method have been used to derive the results of linear and nonlinear stability analysis of this problem, respectively. Both results confirm the stabilizing influence of M and We, and the destabilizing influence of E, Re and θ on this flow dynamics as well. A new feature that emerges from this analysis is the separation of all four distinct (explosive, supercritical, unconditional and subcritical) flow zones in the Re–k, θ–k, M–k and E–k planes, from which one can easily recognize the proper zone of this flow problem under any given values of E, k, M, Re and θ. However, all four distinct flow zones of this problem exist prior to (or next to) the critical value of a stabilized (or destabilized) parameter provided that the curve $J_2 = 0$ does not cross the curve $\omega_i^+ = 0$. Especially in the Re–k plane, for a suitable value of M, dependent on E and θ, the curve $J_2 = 0$ crosses the curve $\omega_i^+ = 0$ for which the unconditional stable zone vanishes at the crossing point (Re_0, k_0). And after the value Re_0, a new (second) explosive unstable zone originates in the flow system, which increases with the increase of Re as well as E and θ. The new information that comes from this analysis is the conditions for the non-existence of an unconditional stable zone, as well as the existence of one or two numbers in the range of k for an explosive unstable zone, which are essentially the relations between k_c and k_j that depend highly on the values of M. Besides this, the existence of two critical values of M are found: one is M_c, which depends on the values of E, Re and θ, while the other is constant, which is $M_j \approx 3.99730$. Finally, we conclude that the destabilizing influence of an electric (or Reynolds number or angle of inclination) parameter on this flow field can be controlled by applying a suitable amount of a magnetic (stabilizing) parameter, depending upon the values of the other parameters related to the problem.

Acknowledgements. We would like to thank the editors and reviewers for their useful comments that helped to improve the quality of the paper. Thanks are also due to Dr J. Dangar, S. Dholey and A. Dholey for their kind cooperation during the work.

Declaration of interests. The authors report no conflict of interest.

Author ORCIDs.
S. Dholey https://orcid.org/0000-0002-8928-6249;
S. De https://orcid.org/0000-0001-8988-3679.

Appendix A

Expressions for L_0, L_1, L_2 and N_2, N_3 are

$$\left.\begin{aligned}
L_0 &\equiv \partial_t + a_1\partial_x + a_2\partial_t^2 + a_3\partial_x\partial_t + a_4\partial_x^2 + a_5\partial_x^4,\\
L_1 &\equiv \partial_{t_1} + a_1\partial_{x_1} + 2a_2\partial_t\partial_{t_1} + a_3(\partial_x\partial_{t_1} + \partial_{x_1}\partial_t) + 2a_4\partial_x\partial_{x_1} + 4a_5\partial_x^3\partial_{x_1},\\
L_2 &\equiv \partial_{t_2} + a_2(\partial_{t_1}^2 + 2\partial_t\partial_{t_2}) + a_3(\partial_x\partial_{t_2} + \partial_{x_1}\partial_{t_1}) + a_4\partial_{x_1}^2 + 6a_5\partial_x^2\partial_{x_1}^2,\\
N_2 &= a_6(\eta_1\eta_{1x}) + a_7(\eta_1\eta_{1t}) + a_8(\eta_1\eta_{1t})_t + a_9(\eta_1\eta_{1x})_x + a_{10}(\eta_1\eta_{1xxx})_x,\\
N_3 &= a_6(\eta_1\eta_{1x_1} + \eta_1\eta_{2x} + \eta_2\eta_{1x}) + a_7(\eta_1\eta_{1t_1} + \eta_1\eta_{2t} + \eta_2\eta_{1t})\\
&\quad + a_8\left\{(\eta_1\eta_{1t_1} + \eta_1\eta_{2t} + \eta_2\eta_{1t})_t + (\eta_1\eta_{1t})_{t_1}\right\}\\
&\quad + a_9\left\{(\eta_1\eta_{1x_1} + \eta_1\eta_{2x} + \eta_2\eta_{1x})_x + (\eta_1\eta_{1x})_{x_1}\right\}\\
&\quad + a_{10}\left\{(\eta_1\eta_{2xxx} + 3\eta_1\eta_{1xxx_1} + \eta_2\eta_{1xxx})_x + (\eta_1\eta_{1xxx})_{x_1}\right\}.
\end{aligned}\right\} \tag{A1}$$

Appendix B

Expressions for the various coefficients present in (4.25) are

$$\left.\begin{aligned}
c_g'(k) &= -\frac{(D_{\omega_r}^2 c_g^2 + 2D_{\omega_r k}c_g + D_k^2)}{D_{\omega_r}},\\
F_r &= \frac{1}{1+(a_3k-2a_2\omega_r)^2}, \quad F_i = \frac{2a_2\omega_r - a_3k}{1+(a_3k-2a_2\omega_r)^2},\\
J_2 &= E_rQ_{1r} - E_iQ_{1i}, \quad J_4 = E_iQ_{1r} + E_rQ_{1i},\\
E_r &= \frac{(a_6k - a_7\omega_r)(a_3k-2a_2\omega_r) - (a_8\omega_r^2 + a_9k^2 - 7a_{10}k^4)}{1+(a_3k-2a_2\omega_r)^2},\\
E_i &= \frac{(a_6k - a_7\omega_r) + (a_3k-2a_2\omega_r)(a_8\omega_r^2 + a_9k^2 - 7a_{10}k^4)}{1+(a_3k-2a_2\omega_r)^2},\\
Q_{1r} &= \frac{MQ_r + NQ_i}{M^2+N^2}, \quad Q_{1i} = \frac{MQ_i - NQ_r}{M^2+N^2},\\
Q_r &= 2a_8\omega_r^2 + 2a_9k^2 - 2a_{10}k^4, \quad Q_i = -(a_6k - a_7\omega_r),\\
M &= 4(-a_2\omega_r^2 + a_3k\omega_r - a_4k^2 + 4a_5k^4), \quad N = 2(a_1k - \omega_r).
\end{aligned}\right\} \tag{B1}$$

References

Alekseenko, S.V., Nakoryakov, V.E. & Pokusaev, B.G. 1994 *Wave Flow of Liquid Films*. Begell House.

Benjamin, T.B. 1957 Wave formation in laminar flow down an inclined plane. *J. Fluid Mech.* **2**, 554–574.

Benney, D.J. 1966 Long waves on liquids films. *J. Math. Phys.* **45**, 150–155.

Binnie, A.M. 1957 Experiments on the onset of wave formation on a film of water flowing down a vertical plane. *J. Fluid Mech.* **2**, 551–553.

Binnie, A.M. 1959 Instability in a slightly inclined water channel. *J. Fluid Mech.* **5**, 561–570.

Blum, E., Mayorov, M. & Tsebers, A. 1989 *Magnetic Fluids*. Zinatne.

Chandrasekhar, S. 1961 *Hydrodynamic and Hydromagnetic Stability*. Dover Publications.

Chang, H.C. 1989 Onset of nonlinear waves on falling films. *Phys. Fluids* **1**, 1314–1327.

Conroy, D. & Matar, O.K. 2017 Dynamics and stability of three-dimensional ferrofluid films in a magnetic field. *J. Engng Maths* **107**, 253–268.

DANDAPAT, B.S. & MUKHOPADHYAY, A. 2003 Finite amplitude long wave instability of a film of conducting fluid flowing down an inclined plane in presence of electromagnetic field. *Intl J. Appl. Mech. Engng* **8**, 379–383.

DHOLEY, S. 2016 Magnetohydrodynamic unsteady separated stagnation-point flow of a viscous fluid over a moving plate. *Z. Angew. Math. Mech.* **96**, 707–720.

DHOLEY, S. 2017 Instabilities of a thin viscoelastic liquid film flowing down an inclined plane in the presence of a uniform electromagnetic field. *Rheol. Acta* **56**, 325–340.

DHOLEY, S. & GORAI, S. 2021 Hydrodynamic instabilities of a viscous liquid film flowing down an inclined or vertical plane. *Phys. Fluids* **33**, 1–19.

FULFORD, G.D. 1964 The flow of liquids in thin films. *Adv. Chem. Engng* **5**, 151–236.

GJEVIK, B. 1970 Occurrence of finite amplitude surface waves on falling liquid films. *Phys. Fluids* **13**, 1918–1925.

GLUKHIKH, V.A., TANANAEV, A.V. & KIRILOV, I.R. 1987 *Magnetohydrodynamics in the Nuclear Energy Systems*. Energoatonizdat.

GONZALEZ, A. & CASTELLANOS, A. 1996 Nonlinear electrohydrodynamic waves on films falling down an inclined plane. *Phy. Rev.* E **53**, 3573–3578.

GREENBERG, A.B. 1956 The mechanics of film flow on a vertical surface. PhD thesis, Purdue University.

ISHIHARA, T., IWAGAKI, Y. & ISHIHARA, Y. 1952 On the roll wave-trains appearing in the water flow on a steep slope surface. *Mem. Fac. Engng Kyoto Univ.* **14**, 83–91.

KAPITZA, P.L. & KAPITZA, S.P. 1949 Wave flow of thin layers of viscous fluid. *Zh. Eksp. Teor. Fiz.* **19**, 105–120.

KORSUNSKY, S. 1999 Long waves on a thin layer of conducting fluid flowing down an inclined plane in an electromagnetic field. *Eur. J. Mech. (B/Fluids)* **18**, 295–313.

LEE, J.J. & MEI, C.C. 1996 Stationary waves on an inclined sheet of viscous fluid at high Reynolds and moderate Weber numbers. *J. Fluid Mech.* **307**, 191–229.

LIN, S.P. 1974 Finite amplitude side-band stability of a viscous film. *J. Fluid Mech.* **63**, 417–429.

LIU, J. & GOLLUB, J.P. 1994 Solitary wave dynamics of film flows. *Phys. Fluids* **6**, 1702–1712.

LIU, J., PAUL, J.D. & GOLLUB, J.P. 1993 Measurements of the primary instabilities of film flows. *J. Fluid Mech.* **250**, 69–101.

MASSOT, C., IRANI, F. & LIGHTFOOT, E.N. 1966 Modified description of wave motion in a falling film. *AIChE J.* **12**, 445–455.

MUKHOPADHYAY, A., DANDAPAT, B.S. & MUKHOPADHYAY, A. 2008 Stability of conducting liquid flowing down an inclined plane at moderate Reynolds number in the presence of constant electromagnetic field. *Intl J. Non-Linear Mech.* **43**, 632–642.

PAPAGEORGIOU, D.T. 2019 Film flows in the presence of electric fields. *Annu. Rev. Fluid Mech.* **51**, 155–187.

PROKOPIOU, T., CHENG, M. & CHANG, H.C. 1991 Long waves on inclined films at high Reynolds number. *J. Fluid Mech.* **222**, 665–691.

PUMIR, A., MANNEVILLE, P. & POMEAU, Y. 1983 On solitary waves running down an inclined plane. *J. Fluid Mech.* **135**, 27–50.

ROHLFS, W., CAMMIADE, L.M.F., RIETZ, M. & SCHEID, B. 2021 On the effect of electrostatic surface forces on dielectric falling films. *J. Fluid Mech.* **906**, A18.

SHERCLIFF, J.A. 1965 *A Textbook of Magnetohydrodynamics*. Pergamon Press.

TSELUIKO, D. & PAPAGEORGIOU, D.T. 2006 Wave evolution on electrified falling films. *J. Fluid Mech.* **556**, 361–386.

WHITAKER, S. & JONES, L.O. 1966 Stability of falling liquid films. Effect of interface and interfacial mass transport. *AIChE J.* **12**, 421–431.

WRAY, A.W., MATAR, O.K. & PAPAGEORGIOU, D.T. 2017 Accurate low-order modeling of electrified falling films at moderate Reynolds number. *Phys. Rev. Fluids* **2**, 063701.

YIH, C.S. 1963 Stability of liquid flow down an inclined plane. *Phys. Fluids* **6**, 321–334.